Ministry of Higher Education and
Scientific Research
University of Baghdad
Institute of Laser for Postgraduate Studies

A comparison Study of Quantum Repeater

A Thesis

Submitted to the Institute of Laser for Postgraduate Studies, University of Baghdad in Partial Fulfillment of the Requirements for the Degree of Master of Science in Laser / Electronic and Communication Engineering

By
Marwa Hameed Kadhim

B.Sc. Communication Engineering - 2007

Supervisor

Dr. Jawad A. K. Hasan

2021 AD **1443 AH**

بِسْمِ اللَّهِ الرَّحْمَنِ الرَّحِيمِ

قَالُوا سُبْحَانَكَ لَا عِلْمَ لَنَا إِلَّا مَا عَلَّمْتَنَا إِنَّكَ أَنْتَ الْعَلِيمُ الْحَكِيمُ.

صدق الله العلي العظيم

سورة البقرة - الاية 32

Certification

I certify that this thesis was prepared under my supervision at the Institute of Laser for Postgraduate Studies, University of Baghdad, as a partial fulfillment of requirements for the degree of "Master of Science in Laser/ Electronic and Communication Engineering".

Signature:

Name: **Dr. Jawad A. K. Hasan**

Title: Lecturer

Address: Institute of Laser for Postgraduate studies,
University of Baghdad.

Date: / / 2021
(Supervisor)

In view of the available recommendation, I forward this thesis for debate by Examining Committee.

Signature:

Name: **Asst. Prof. Dr. Hanan Jaafar Taher**

Title: Head of the Scientific Committee.

Address: Institute of Laser for Postgraduate studies,
University of Baghdad.

Date: / /

Examination Committee Certification

We certify that we have read this thesis " A comparison Study of Quantum Repeater " and as Examination Committee, we examined the student in its content and in our opinion, it is adequate with standards as a thesis for a degree of Master in science in Laser /Electronic and Communication Engineering.

Signature:
Name:
Title:
Address:
Date: / / 2021
(Chairman)

Signature:
Name:
Title:
Address:
Date: / / 2021
(Member)

Signature:
Name:
Title:
Address:
Date:
(Member)

Signature:
Name
Title:
Address: .
Date: / / 2021
(Supervisor)

Approval by the Deanship of Institute of Laser for Post graduate Studies, University of Baghdad.

Signature:
Name:
Title:
Address:
Date: / / 2021

ACKNOWLEDGEMENTS

First and foremost, I am grateful to the creator ***"ALLAH"*** for giving me the strength, enablement, knowledge and understanding required to complete this work. I am heartily thankful to my supervisor, ***Dr. Jawad A. K. Hassan***, whose encouragement, invaluable guidance and kind support. His broad knowledge and clear thought inspired me; from the initial to the final level enabled me to develop and understand the project. I would like to thank ***Prof. Dr. Hussein A. Jawad***, the Dean of Institute of Laser for Postgraduate Studies. Special thanks also go to all the members of ***Photonic Department*** for their help and encouragement. I wish to express my deepest love to my Family. Thanks for your endless Support for me when I feel frustrated during the study.

الإهداء....

الى رمز الطيبة .... الى من أحمل اسمه بكل فخر .... والصدق

الى من رحل من عالمنا وما زال ً دوي نصائحه يوجهني..

أبي رحمه الله برحمته الواسعه

الى من قدمت سعادتي .... وراحتي على سعادتها.. الى من كان دعائها سر نجاحي

الى معنى الحب والحنان..

أمي الفاضله ....

ألى زوجي الذي ساندني بكل مجالات الحياه

ألى أولأدي (أسحاق . سلسبيل. بسمله) الذين هم زهرة حياتي

الى أخواني و أخواتي اللواتي يشاركوني الفرح والحزن

الى مشرفي العزيز.. الذي كان نورا يضيء الظلمه التي كانت تقف احيانا في طريقي

الى من زرعوا التفاؤل في دربي وقدموا لي المساعده والأفكار والمعلومات .

أساتذتي ،أهلي وأصدقائي فلهم مني كل الشكر

الى كل من يحبني بصدق وإخلاص ..... إن إنهائي عملي لم يكن ليتم لولا دعمكم ،أتمنى ان ينال رضاكم ومن الله عز وجل ...

Abstract

Sending information for long distances in communication systems suffers from the exponential decay of the signals in both optical fiber and free space channels, hence, to overcome such problem a quantum repeater is introduced. In this research, a study of the effect of both decoherence time (life time T_2) and coupling efficiency (η_c) on the performance of the quantum repeater in both single and multi-node cases is presented. Also, a comparison between quantum system and hybrid system is presented. Therefore, different quantum memories with different decoherence time and coupling efficiency were used to examine its effect on the performance of both single and multi-node quantum repeater. The results shows that as the decoherence time of the quantum memory become longer the distance that the data can reach is increased without any effect on the key rate amount, in which, for (T_2= 16 sec distance reached is about 900km), while for (T_2= 0.018 sec distance reached is about 400km) . Also, increasing coupling efficiency will affected both distance and key rate especially in multi-node quantum repeater. Finally, the results of the comparison between quantum and hybrid systems states that quantum system case has scored higher bit rate as their channel is purely optical or wireless with high bandwidth, which increases the data rate. In the hybrid case, part of the channel has been a classical wireless, which has less bandwidth than the all quantum case. Finally, the all classical case has lower frequency and bandwidth that forces the data rate to become the least. Also, The obtained outcome shows the hybrid systems may provide reduced delay, less maintenance and maximized scalability.

List of Contents

List of Figures

List of Tables

List of Abbreviations

cbit	classical bit
qbit	quantum bit
QKD	quantum key distribution
ASCII	American Standard Code for Information Interchange
NRZ	return to zero
RZ	non return to zero
NRZ-I	non return to zero inventive
H gate	hadamard gate
CNOT	controlled NOT gate
POVM	positive operator valued measure
DLCZ	Duan-Lukin-Cirac-Zoller
QR	quantum repeater
QM	quantum memory
DAC	digital-to-analogue converters
ADC	analogue-to-digital converters
AWG	arbitrary waveform generators
Amps	amplifiers
MUX	multiplexers
ASIC	Application specific integrated circuits
FPGA	field-programmable gate arrays
QBER	quantum bit error rate

List of Symbols

$\lvert\psi\rangle$	vector space
ψ	label for the vector
$\sigma_x, \sigma_y, \sigma_z$	Pauli matrices in x, y, z
α_0 , α_1	complex numbers
η_d	detection efficiency
p_{dark}	dark count probability
η_p	quantum memory preparation efficiency
T_{prep}	quantum memory preparation time
η_c	coupling efficiency
η_{ch}	transmission efficiency of light in a fiber
L_{att}	attenuation length
η_λ	wavelength conversion efficiency
η_{tot}	total efficiency
e_M	misalignment parameter (error)
L	channel length
L_i, L_a, L_b	Inner and outer lengths
x, y	spiacing parameter
n	number of nodes
p_{BSM}	Bell state measurement success probability
p_{OBSM}	optical Bell state measurement success probability
η_{inner}	transmission efficiency of light in the inner links
γ	mode- mismatch
$e_{obsm,x}$, $e_{obsm,z}$	probability of an error happening in the optical Bell state measurement in X and Z bases
R	key rate

Y	yield
f	inefficiency
e_x, e_z	quantum bit error rate in X and Z bases
P_a	probability of success in Alice's external link
P_b	probability of success in Bob's external link
P_i	probability of success in inner links
$\eta_{a,b}$	efficiency in Alice and Bob side
$f_{dp}[n]$	memory dephasing parameter
τ_i	repetition rate of a trial for each link
τ_p	repetition rate of a trial for inner link
τ_b	repetition rate of a trial for outer link
T_i	quantum memory storage time
t_i	node waiting time (success time)

Chapter One

Background & Literature Review

1.1 Overview

Quantum computing has been the most interesting and promising technology to provide solutions to problems that are not easy to solve using classical communications. This can be done without tradeoffs so as the utilization of quantum a network becomes complete. Recently, the quantum entangled photons are suggested as the quantum states to be transmitted to the other sides of the network, for example from Alice to Bob. That is one photon is sent to Alice, the other photon is sent to Bob. When the two sides of the network make some changes on the state of one photon, the other one will respond at the same time. Unless the optical fiber is used to convey this piece of information, it can be lost very efficiently in the atmosphere, when it is sent using wireless channel. Even while using the optical fiber, there are several types of losses that can be imposed on the signal which makes receiving such information is very difficult. As a solution, quantum repeaters have been suggested to solve the limitations of the distance. This technology has suggested using more than entanglement sources while holding the correlation between the photons at the two participants, Alice and Bob.

1.2 Limitation of Classical Communication

In today's communication systems, the important information is commonly encrypted and afterward sent across fiber-optic links or any another channels along with the secrete keys needed for decoding the information. Both information and keys are send in the form of classical bits representing a stream of optical or electrical signal representing logical pulses 0s and 1s. which make them weak and easy to be hacked by hackers, who can read and copy these keys without leaving any trace. So to avoid this case, a quantum communication is presented which use the laws of quantum mechanics to protects information from being hacked. The laws of quantum mechanics allows particles which is represented by photon of light to be transmitted across the optical fiber to take on a state of superposition, in which multiple 0 and 1 combinations can be represented simultaneously. Such kind of particles are known as quantum bits (qbits) [1].

Quantum communications exploits the laws of quantum Mechanics science to secure the transmission of information. These laws permit particles commonly photons of light for communicating information along optical links to take on a condition of superposition, which implies they can address numerous blends of 1 and 0 all the while. The particles are known as quantum bits, or qubits. The excellence of qubits according to cyber-security viewpoint is that if an eavesdropper attempts to observe them on the way, their super fragile quantum state "falls" to 0 or 1. This implies that eavesdropper can't alter the qubits without leaving behind an indication. A few organizations enjoy taken benefit of this property to make networks for communicating exceptionally delicate information dependent on a cycle called quantum key distribution, or QKD [2].

1.3 Classical Information

Classical information is represented as a series of separate symbols that each of which can take just one of a limited number of values, like digits or letters. Claude Shannon is the first scientist who defined classical information [3]. Binary data represent the most common form digital (classical) data in modern information systems that is represented by a string of bits, where each of these bits can take one of just two values 0 or 1[4].

1.3.1 Classical Bits (Cbit)

Binary numbers are positional numeral system with a base on powers of two, which is consists of just two logical values one and zero that used to represents all other numbers. And, because of its easy implementation in logic gates, its used widely in computer based devices, digital signal processing, and networking. Binary numbers are known as bits or (classical bits) which can be taken the logical values 0 or 1 only [5].

Classical bits are used to represents data as a sequence of discrete values at any time in contrast with the analog signal which is represented by continuous values physically. These two values represent two voltage bands, For example in TTL one of them is near the supply voltage which almost (+5 v) referred to bit (1) while the other is the zero volt (0 v) or ground which represent bit (0). Also it can be represent as (High and Low), (True and False) as shown in figure (1.1) [6].

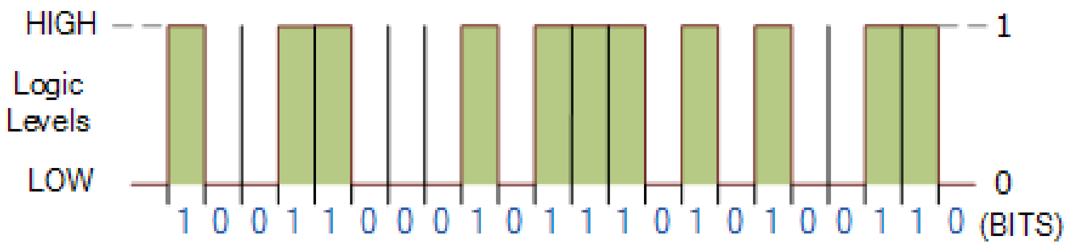

Fig. 1.1. Classical bit representation

1.4 Quantum Mechanics

Quantum mechanics is mathematical representation and interpretation of any physical theories. It doesn't tell us what rules this system obey. The four postulates of quantum mechanics give an association between the mathematical formalism of quantum mechanics and the physical system. The postulates of quantum mechanics determined after long procedure of trials and errors, that included lot of searching and guessing by the originators of the theory. The quantum mechanics postulates with the support of density operators can be summarized as follows: [7]

Postulate 1: The state space, related to any physical system which is a complex vector space with inner product ($Hilbert\ space\ H$) known as the state space of the system. The state vector is entirely describing the state of its system, which is a unit vector in the system's state space as:

$$|\psi\rangle = \alpha_0|0\rangle + \alpha_1|1\rangle \quad \ldots\ldots\ldots\ldots\ldots\ldots\ldots \ (1.1)$$

Postulate 2: The evolution of any closed quantum system described by the unitary transformation. In which states $|\psi\rangle$ and $|\psi'\rangle$ in times t1 and t2 respectively are connected by the unitary operator U, which is related to these times only:

$$|\psi'\rangle = U|\psi\rangle \quad \ldots\ldots\ldots\ldots\ldots\ldots\ldots\ldots\ldots \ (1.2)$$

Schrodinger equation describes the time evolution of the quantum system state:

$$i\hbar \quad \frac{\partial}{\partial t}|v\rangle = \mathcal{H}\ |v\rangle \quad \ldots\ldots\ldots\ldots\ldots\ldots\ldots\ldots\ldots \ (1.3)$$

Where: $\hbar$ is the reduced Planck constant, $\hbar \approx 1.055 \times 10^{-34}$ Js. And $\mathcal{H}$ is a stable Hermitian operator called the Hamiltonian of the system. Actually, it is an appropriate to absorb $\hbar$ into $\mathcal{H}$, effectually setting $\hbar$ = 1. The Schrodinger equation solution's (1.20) establishes an operator of time evolution is [7]:

$$U(\Delta t) = e{-}iH\Delta t \quad \ldots\ldots\ldots\ldots\ldots\ldots\ldots\ldots\ldots \ (1.4)$$

The operator of time evolution is $U(\Delta t)$, it is a unitary operator since the Hamiltonian $\mathcal{H}$ is a Hermitian matrix, $\mathcal{H} = \mathcal{H}\dagger$, thus the unitarity condition is satisfied as [7]:

$$U\ (\Delta t)U\ (\Delta t)_{\dagger} = e{-}iH\Delta t\ eiH\Delta t = I\ \ldots\ldots\ (1.5)$$

The second postulate can reformulate utilizing unitary evolution as: The closed quantum system time evolution of the state $|v_1\rangle$ at time $(t1)$ to the state $|v2\rangle$ at time ($t2$) is defined using a unitary operator $U = U\ (t_2 - t_1)$ [7]:

$$|v_2\rangle = U\ |v_1\rangle\ \ldots\ldots\ldots\ldots\ldots\ldots\ldots\ldots\ldots\ldots\ (1.6)$$

Postulate 3: Quantum measurement, $\{M_m\}$ represents the assembly of the quantum measurement operators. The measurement operators can be performed on the state space of the system demanded to be measured.. The system state $|v\rangle$ measured may give as [7]:

$$P\ (r_m) = \langle v|M_m \dagger\ M_m|v\rangle\ \ldots\ldots\ldots\ldots\ldots\ldots\ (1.7)$$

The system state $|v\rangle$ outcome is rm with probability $P\ (rm)$. the index m denotes to the measurement result rm which may arise in the experiment. So, the state of the system after measurement is [7]:

$$|v'\rangle = \frac{M_m|v\rangle}{\sqrt{P(r_m)}}\ \ldots\ldots\ldots\ldots\ldots\ldots\ldots\ldots\ (1.8)$$

The operators $\{M_m\}$ satisfy the completeness equation:

$$\sum_m M_m^{\dagger} M_m = I\ \ \ldots\ldots\ldots\ldots\ldots\ldots\ldots\ldots\ (1.9)$$

Utilizing the completeness equation (1.9) composed with the normalization condition, their probabilities sum is one [7]:

$$\sum_m P(r_m) = \sum_m \langle v|M_m^{\dagger} M_m|v\rangle = 1\ \ldots\ldots\ (1.10)$$

A projective measurement P_m tolerates to state the measurement, in an orthonormal basis $|m\rangle$ principally as [7]:

$$P_m = |m\rangle\langle m| \quad \ldots\ldots\ldots\ldots\ldots\ldots\ldots\ldots\ldots.. \quad (1.11)$$

Postulate 4: Composite systems: tensor product of the subsystems states spaces represents the composite system state. If the state space S of the tensor product of the state spaces S_i of composite physical system, then its constituents are [7]:

$$S = \otimes_i S_i \quad \ldots\ldots\ldots\ldots\ldots\ldots\ldots\ldots\ldots. \quad (1.12)$$

Additionally, if the sub-systems are in the states $|vi\rangle \in Si$, later the joint state $|v\rangle \in S$ of the entire system is [8]:

$$|v\rangle = \otimes_i v_i \quad \ldots\ldots\ldots\ldots\ldots\ldots\ldots\ldots\ldots.. \quad (1.13)$$

1.5 Quantum Information

Quantum information referred to the information of the quantum system. It represent the main object of study in the theory of quantum information, and can be employed using processing techniques of quantum information. It denotes to both technical definition of Von Neumann entropy and general computational term [8].

Quantum information an interdisciplinary field comprises of many subjects such as quantum mechanics, information theory, computer science, cryptography, philosophy [9], as well as, cognitive science, neuroscience and psychology. The main aim of quantum information is to extract information from substance at a microscopic scale. Observation is the best method for obtaining information, whereas measurement is important so as to quantify observation. In quantum mechanics, according to the uncertainty principle, non-commuting observables cannot be exactly measured simultaneously since the eigenstate cannot be the same in two different places, hence, a quantum state can never comprise complete information about both variables [10].

In physics data is encoded in the state of quantum system, whereas, quantum mechanics focuses on investigating the characteristics of substances at a microscopic scale, the science of quantum information aims to obtain data from these characteristics, and quantum computation deal with these data to accomplishes the desired logical operations [11]. Quantum information like classical information, can be manipulated using digital computers, transmitted between two distant locations. The field of quantum information and quantum computing become recently an active area of research because of its different applications in communications and cryptography [12].

1.6 Quantum Bit (Qubit)

In quantum computing, a qubit or quantum bit is the basic unit of quantum information and the quantum version of the classical binary bit physically realized with a two-state device. A qubit is a two-state level quantum system. The qubit, physically can be represented by the time bin encoding , the polarization of a single photon in which the two states can be taken to be the vertical polarization and the horizontal polarization or the spin of the electron in which the two levels can be taken as spin up and spin down. In a classical system, a bit would have to be in one state or the other such as (0 or 1) [13].

However, quantum mechanics allows the qubit to be in a coherent superposition of both states/levels simultaneously, a property which is fundamental to quantum mechanics and quantum computing. The basic data unit in a classical communication is the bit (0 or 1). while in quantum computation, a quantum bit is used that can be in a superposition state, which is shortened to qubit (0 and 1). Superposition states allow many computations to be performed simultaneously, and gives rise to what is known as quantum parallelism. Quantum parallelism is an important property of quantum computing. It is based on using the calculations that are superposition of the base states that can simultaneously produce a large number of calculations with various input data. A quantum superposition state allows a qubit to store (0 and 1) simultaneously. Two qubits can store all the 4 binary numbers 00, 01, 10 and 11 simultaneously. Three qubits stores the 8 binary numbers 000, 001, 010, 011, 100, 101, 110 and 111 simultaneously and so on as binary numbers = $2N$, where N = qubit number [13].

So, what is the qubit?

- The quantum bit (qubit) is the smallest quantum information unit.
- Qubits are often made of subatomic particles such as:
  - Photons
  - Coherent state of light
  - Electrons
  - Quantum dot
  - Optical lattice

The problems related with the qubit:

- Observer effect
  - Qubit cannot be observed without destroying their state.
- Decoherence
  - Decoherence occurs when a system interacts with its environment.

A single qubit can be described by a vector two dimensional complex Hilbert space. Also, qubits can be represented by an arbitrary superposition of twostate system as:

$$|\psi\rangle = \alpha|0\rangle + \beta|1\rangle \quad \ldots\ldots\ldots\ldots\ldots\ldots\ldots\ldots\ldots\ (1.14)$$

Where, $|1\rangle$ and $|0\rangle$ represent any orthonormal basis in the state space, and α, β are complex numbers, called amplitudes, associated with the basis states, the qubit state vector must have unit norm, $|\alpha|2 + |\beta|2 = 1$.

In quantum mechanics, the Bloch sphere as shown in Fig. (1.2), is a geometrical representation of the qubit. Given an orthonormal basis, any pure state $|\psi\rangle$of a two-level quantum system can be written as a superposition of the basis vectors $|1\rangle$ and $|0\rangle$. From quantum mechanics that the total probability of the system has to be one: $\langle\psi|\psi\rangle = 1$, where $|\psi\rangle$ can rewrite the qbit as [13]:

$$|\psi\rangle = \cos\left(\frac{\theta}{2}\right)\ |0\rangle + e^{i\varphi}\sin\ \left(\frac{\theta}{2}\right)|1\rangle \quad \dots\dots\dots (1.15)$$

Where: $(0 \leq \theta \leq \pi)$ and $(0 \leq \varphi \leq 2\pi)$.

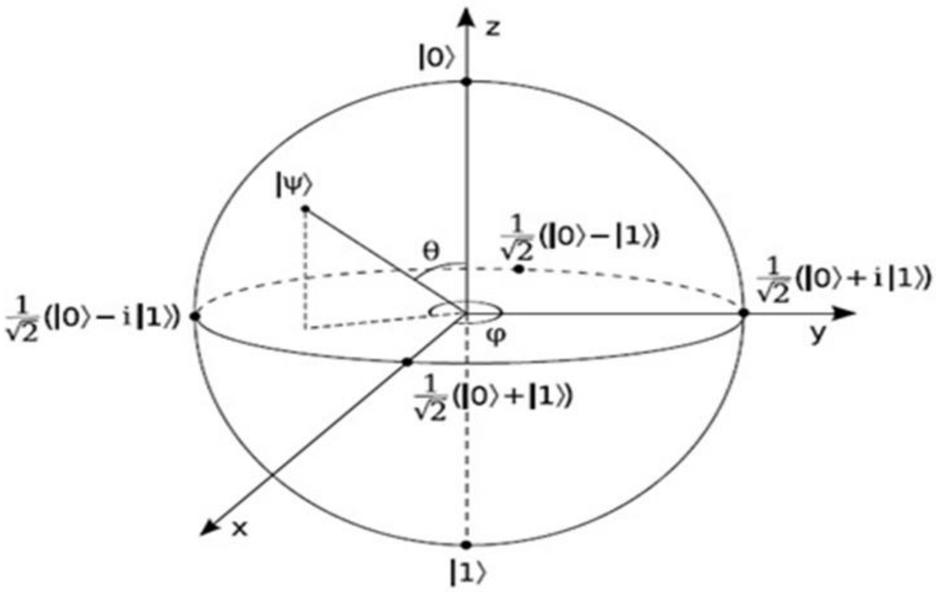

Fig. 1.2: The representation of qubit on Bloch sphere. The state of the qubit can be defined by the angles that create a unit vector that points from the origin to the surface of the sphere $|\psi\rangle = \alpha|0\rangle + \beta|1\rangle = \cos\left(\frac{\theta}{2}\right)\ |0\rangle + e^{i\varphi}\sin\ \left(\frac{\theta}{2}\right)|1\rangle$. θ determines the relative amplitudes of the two basis states while φ defines the phase between the two components of the vector [14].

The qubit, physically can be represented by, time bin encoding that is a technique used in quantum information science to encode a qubit of information on a photon, spin directions of an electrons in the magnetic field, or individual polarization states of a photon. The related state space of two dimensional complex Hilbert space $H2$, that is crossed by an orthonormal basis $\mathcal{B} = \{|1\rangle, |0\rangle\}$. The $|1\rangle$ *and* $|0\rangle$ raises to the typical (computational) basis well-defined as [13]:

$$|0\rangle = \binom{1}{0} \; and \; |1\rangle = \binom{0}{1} \longrightarrow \text{(standard basis)}$$

The tensor product of the individual sub-system states represent the combined state of a composed system. If the two $qubits$ $|v\rangle, |\varphi\rangle \in H2$, $|v\rangle = \alpha|0\rangle + \beta|1\rangle$, $|\varphi\rangle = \gamma|0\rangle + \delta|1\rangle$. Their tensor product is equal to [14]:

$$|v\rangle|\varphi\rangle = \alpha\gamma|0\rangle|0\rangle + \alpha\delta|0\rangle|1\rangle + \beta\gamma|1\rangle|0\rangle + \beta\delta|1\rangle|1\rangle \; ..... \; (1.16)$$

This equation can be written as [13]:

$$|v\rangle|\varphi\rangle = \alpha_{00}|00\rangle + \alpha_{01}|01\rangle + \alpha_{10}|10\rangle + \alpha_{11}|11\rangle = \Sigma_{i\in\{0,1\}2}\, \alpha_i|i\rangle \; (1.17)$$

States: $|00\rangle, |01\rangle, |10\rangle$ *and* $|11\rangle$ are the typical basis vectors of Hilbert space H as [13]:

$$|00\rangle = \binom{1}{0} \bigotimes \binom{1}{0} = \begin{pmatrix}1\\0\\0\\0\end{pmatrix}, \qquad |01\rangle = \binom{1}{0} \bigotimes \binom{0}{1} = \begin{pmatrix}0\\1\\0\\0\end{pmatrix},$$

$$|10\rangle = \binom{0}{1} \otimes \binom{1}{0} = \begin{pmatrix}0\\0\\1\\0\end{pmatrix}, \qquad |11\rangle = \binom{0}{1} \otimes \binom{0}{1} = \begin{pmatrix}0\\0\\0\\1\end{pmatrix}$$

The (00, 01, 10, 11) can be named again to (0, 1, 2, 3) since they can be simply seen as a binary symbol of these integers [13].

An example of a qubit as a photon (a particle of light) travelling along two possible paths. Consider what happens when a photon encounters a beam splitter as shown in Figure (1.3). A beam splitter is just like an ordinary mirror, however the reflective coating is made so thin that not all light is reflected and some light is transmitted through the mirror as well. When a single photon encounters a beam splitter, the photon emerges in a superposition of the reflected path and the transmitted path. One path is taken to be the binary number 0, and the other path is taken to be the number 1. The photon in a superposition of both paths and so represents both 0 and 1 simultaneously [14].

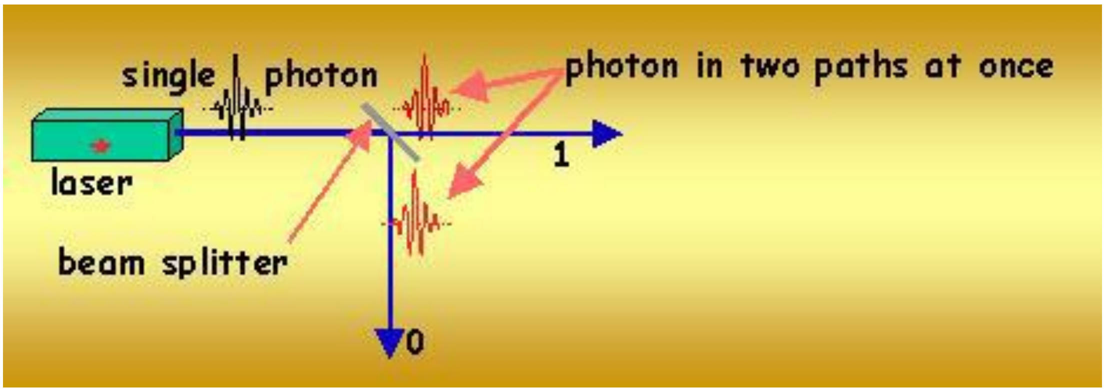

Fig. 1.3: A qubit as a photon (a particle of light) travelling along two possible paths when a photon encounters a beam splitter [14].

However, photons which can be provided from laser source are ideal carriers for quantum information processing and quantum communication since they are easy to be generated and manipulated. But, the most important problem is that photons suffer from that they can not be stored and experience losses during the transmission [15].

1.7 Quantum Gates

Quantum gates can be considered as an elementary quantum computing device which execute a fixed unitary operation on desired Qbits in a fixed timeframe. Quantum logic gates are reversible as compared with the classical logic gates. It is conceivable to implement classical computing using just quantum gates as in Toffoli gate [2]. Density matrices are used to validate quantum gates [8].

In the next paragraphs, the operation and characteristics of some quantum gates will be introduced [2].

1. Pauli-X or bit-flip gate

$$|\psi\rangle = X\ |\phi\rangle = \begin{bmatrix} 0 & 1 \\ 1 & 0 \end{bmatrix}\begin{bmatrix} a \\ b \end{bmatrix} = \begin{bmatrix} b \\ a \end{bmatrix} \equiv b\,|0\rangle + a|1\rangle \quad \ldots\ldots\ldots\ldots\ldots\ldots\ldots\ldots\ldots\ldots\ldots(1.17)$$

It's clear that, this gate exchanges the computational basis states probability amplitudes. Considering the classical case $|\varphi\rangle = |0\rangle$ or $|1\rangle$, $|\psi\rangle$ is inverse of $|\varphi\rangle$.

2. Pauli-Z or phase-flip gate

$$|\psi\rangle = Z\ |\phi\rangle = \begin{bmatrix} 1 & 0 \\ 0 & -1 \end{bmatrix}\begin{bmatrix} a \\ b \end{bmatrix} = \begin{bmatrix} a \\ -b \end{bmatrix} \equiv a\,|0\rangle - b\,|1\rangle \quad \ldots\ldots\ldots\ldots\ldots\ldots\ldots\ldots\ldots\ldots(1.18)$$

The phase of second amplitude is shifted by 180^0 (π).

3. Pauli-Y gate

$$|\psi\rangle = Y\ |\phi\rangle = \begin{bmatrix} 0 & -j \\ j & 0 \end{bmatrix}\begin{bmatrix} a \\ b \end{bmatrix} = \begin{bmatrix} -jb \\ ja \end{bmatrix} \equiv -jb\,|0\rangle + ja|1\rangle \quad \ldots\ldots\ldots\ldots\ldots\ldots\ldots\ldots(1.19)$$

Its operation is to shift the phase between the initial and final state by $(\pi/2)$.

The operation of Pauli gates may be visualized using Bloch sphere. The aim of using Pauli gates is to make rotation around the X, Y, Z axes. Rotation around the x axis by an angle α can be uttered as:

$$e^{-i\frac{\alpha}{2}X} = \cos(\frac{\alpha}{2})I - i\,\sin(\frac{\alpha}{2})X \quad \ldots\ldots\ldots\ldots\ldots\ldots\ldots\ldots\ldots\ldots\ldots\ldots(1.20)$$

4. Phase-rotator or phase gate

$$|\psi\rangle = P\,|\phi\rangle = \begin{bmatrix} 1 & 0 \\ 0 & e^{j\alpha} \end{bmatrix}\begin{bmatrix} a \\ b \end{bmatrix} = \begin{bmatrix} a \\ e^{j\alpha}b \end{bmatrix} \equiv a\,|0\rangle + e^{j\alpha}b\,|1\rangle \ldots\ldots\ldots\ldots\ldots\ldots\ldots\ldots(1.21)$$

This quantum logic gate characterizes the elementary quantum gate of a simple sheet of glass.

5. Hadamard gate (H)

$$|\psi\rangle = H\,|\phi\rangle = \frac{1}{\sqrt{2}}\begin{bmatrix} 1 & 1 \\ 1 & -1 \end{bmatrix}\begin{bmatrix} a \\ b \end{bmatrix} = \begin{bmatrix} \frac{a+b}{\sqrt{2}} \\ \frac{a-b}{\sqrt{2}} \end{bmatrix} \equiv \frac{a+b}{\sqrt{2}}|0\rangle + \frac{a-B}{\sqrt{2}}|1\rangle \ldots\ldots\ldots\ldots\ldots(1.22)$$

As the H gate acts on single qbit, the state $|0\rangle$ will be mapped to $\frac{|0\rangle+|1\rangle}{\sqrt{2}}$ while the state $|1\rangle$ will be mapped to $\frac{|0\rangle-|1\rangle}{\sqrt{2}}$. So, this leads to that, the measurement have equal probabilities to be in state $|1\rangle$ or $|0\rangle$.

The matrix demonstration of Hadamard gate is as follows:

$$H = \frac{1}{\sqrt{2}}\begin{bmatrix} 1 & 1 \\ 1 & -1 \end{bmatrix}$$

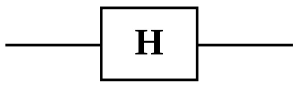

Circuit representation of Hadamard gate

Hadamard gate indicates a single qbit explanation of the quantum Fourier transform, as $HH^* = I$.

In addition to 1–qbit quantum gates, there are several 2-qbits and 3-qbits quantum gates, as illustrated below [2].

1. Controlled (cX cY cZ) gates

These gates act on two or more qbits, in which one or more qbits operate as a control in some cases. The controlled NOT gate (CNOT or cX) represent the important type of such gates, act on 2 qbits. If first qbit is $|1\rangle$, then NOT operation performed on second qbit, otherwise does nothing. The matrix representation of CNOT is shown below:

$$CNOT = cX = \begin{bmatrix} 1 & 0 & 0 & 0 \\ 0 & 1 & 0 & 0 \\ 0 & 0 & 0 & 1 \\ 0 & 0 & 1 & 0 \end{bmatrix}$$

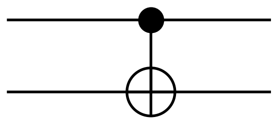

Circuit representation of controlled NOT gate

If generally, U operates on single qubit with matrix representation as illustrated below [11]:

$$U = \begin{bmatrix} u_{00} & u_{01} \\ u_{10} & u_{11} \end{bmatrix}$$

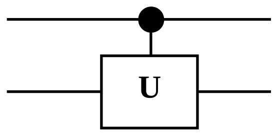

Circuit representation of controlled U-gate

2. Toffoli (CCNOT) gate

This gate represent a three-qbit gate used for classical computation. Its mechanism is as follows. As first two qbits are in state $|1\rangle$, then a Pauli-X (or NOT) is performed on the third bit, otherwise it does nothing. The Toffoli gate can be imagined like the quantum analog of a classical gate. The truth table of Toffoli gate is shown below (table 1.1) [8].

Table 1.1. Toffoli gate truth table

Input			Output		
0	0	0	0	0	0
0	0	1	0	0	1
0	1	0	0	1	0
0	1	1	0	1	1
1	0	0	1	0	0
1	0	1	1	0	1
1	1	0	1	1	1
1	1	1	1	1	0

$$\begin{bmatrix} 1 & 0 & 0 & 0 & 0 & 0 & 0 & 0 \\ 0 & 1 & 0 & 0 & 0 & 0 & 0 & 0 \\ 0 & 0 & 1 & 0 & 0 & 0 & 0 & 0 \\ 0 & 0 & 0 & 1 & 0 & 0 & 0 & 0 \\ 0 & 0 & 0 & 0 & 1 & 0 & 0 & 0 \\ 0 & 0 & 0 & 0 & 0 & 1 & 0 & 0 \\ 0 & 0 & 0 & 0 & 0 & 0 & 0 & 1 \\ 0 & 0 & 0 & 0 & 0 & 0 & 1 & 0 \end{bmatrix}$$

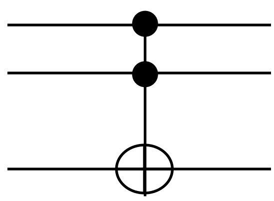

Circuit representation of Toffoli gate

1.8 Quantum Measurement

In quantum physics, measurement refers to manipulation or testing process of a physical system so as to produce a numerical outcome. Quantum physics predictions are always probabilistic, the tools used for prediction the outcomes of measurement were developed throughout the 20th century and make use of both functional analysis and linear algebra. Each physical system in quantum mechanics is associated with a Hilbert space, each element of which is a wave function which signifies a probable state of that physical system. The first measurement method upon a physical system by using a self adjoint operator on a Hilbert space was confined by Neumann and known as "observable"[16].

According to third postulate of quantum mechanics, the measurement can be illustrated by use of a set of operators $\{M_m\}$, where m represents the possible results of measurement. If the physical system in state v, then probability of measuring m can be calculated using Eq. (1.23) [17].

$$p(m/v) = v^{+}M_m^{+}M_m v \quad \ldots\ldots\ldots\ldots\ldots\ldots\ldots\ldots\ldots \; (1.23)$$

Then, after measuring m, the system goes to state Eq. (1.24)

$$v' = \frac{M_m v}{\sqrt{v^{+}M_m^{+}M_m v}} \quad \ldots\ldots\ldots\ldots\ldots\ldots\ldots\ldots\ldots\ldots\ldots \; (1.24)$$

Since the classical probability theory must satisfy that:

$$\sum_m p(m/v) = \sum_m v^{+}M_m^{+}M_m v \equiv 1 \quad \ldots\ldots\ldots\ldots\ldots\ldots \; (1.25)$$

Hence, measurement operator must agrees with following completeness relation:

$$\sum_m M_m^{+}M_m \equiv I \quad \ldots\ldots\ldots\ldots\ldots\ldots\ldots\ldots\ldots\ldots\ldots \; (1.26)$$

It's important to remember that the completeness relation must be checked, as all the measurement operators are assumed to be constructed, as it averts us from forgetting any of the potential measurement results on the measurement equipment indicator dial.

finally, it is clearly that repeated measurements may be combined. Hence, if any measurement such as $\{M_m\}$ is followed by another measurement like $\{Q_q\}$, then these two measurements may be combined with one measurement with operators:

$$R_{qm} = M_m Q_q, \qquad \forall q, m \quad \ldots\ldots\ldots\ldots\ldots\ldots\ldots\ldots \text{(1.27)}$$

All the above definitions do not show us how to make a measurement , they just tell us how to predict the result of a measurement and the system post measurement state. Therefore, it is important to construct our measurement devices as it will be illustrated below.

- **Projective measurement**

The von Neumann eigenvectors make an orthonormal basis for Hilbert space, the each possible results of such measurement belongs to one of the vectors comprising the basis. So to compute the probability distribution over the results of such measurement, a density operator can be used, which is positive-semidefinite operator on the Hilbert space. The trace of density operator equal to one [16,17]. This can be don't through Born rule which states:

$$p(x_i) = tr(\prod_i \rho) \ldots\ldots\ldots\ldots\ldots\ldots\ldots\ldots\ldots\ldots\ldots\ldots \text{(1.28)}$$

Where, ρ is the density operator, and $\prod_i$ is the projection operator onto the basis vector according to the measurement result $\mathbf{x}_i$. The average of a von Neumann eigenvalues observable by using Born-rule probabilities, represents the expectation value of that observable. Hence, for an observable $\mathbf{A}$ the expectation value given a quantum stat ρ is:

$$\langle A \rangle = tr(A\rho) \ldots\ldots\ldots\ldots\ldots\ldots\ldots\ldots\ldots \text{(1.29)}$$

Any density operator that is a rank-1 projection is known as a pure quantum state, and all quantum states that are not pure are known as mixed. Pure states are also known as wave functions. Assigning a pure state to a quantum system implies certainty about the outcome of some measurement on that system (i.e., P (x) = 1} for some outcome x Any mixed state can be written as a convex combination of pure states, though not in a unique way. The state space of a quantum system is the set of all states, pure and mixed, that can be assigned to it [18].

- **Generalized measurement (POVM)**

a positive-operator-valued measure (POVM) is a measure with a positive semi-definite operators value on a Hilbert space. POVMs are a generalization of projection-valued measures (PVMs) and therefore, any quantum measurements described by POVMs are a generalization of quantum measurement described by PVMs. In rough analogy, a POVM is to a PVM what a mixed state is to a pure state. Mixed states are needed to specify the state of a subsystem of a larger system; analogously, POVMs are important to describe the effect on a subsystem of a projective measurement performed on a larger system. POVMs are the most general kind of measurement in quantum mechanics, and can also be used in quantum field theory. They are extensively used in the field of quantum information [19].

1.9 Quantum Entanglement

Quantum entanglement is very important in quantum information theory. since, numerous classically absolutely unimaginable outcomes may be accomplished by quantum information theory. Also, quantum communications based on entanglement become more resistant to noise inherent by a quantum channel, and expand the capacities of quantum channels. Also, based on entanglement, various quantum algorithms have been formed, like, teleportation protocol, and superdense coding [8].

In General, entangled quantum states cannot decompose into tensor product form. The entangled states related to non-local correlation between the particles and does not has a classical correspondent [20].

1.10 Bell States

Bell states are the basic demonstration of the 2 particle maximally entangled state. The quantum circuit used to create a Bell state is shown in figure (1.5), which involves of H gate followed by CX gate. This circuit converts the four computational basis states according to table (1.2) [8].

$$|\beta_{00}\rangle = \frac{|00\rangle + |11\rangle}{\sqrt{2}} \quad \ldots\ldots(1.30)$$

$$|\beta_{01}\rangle = \frac{|01\rangle + |10\rangle}{\sqrt{2}} \quad \ldots\ldots(1.31)$$

$$|\beta_{10}\rangle = \frac{|00\rangle - |11\rangle}{\sqrt{2}} \quad \ldots\ldots(1.32)$$

$$|\beta_{11}\rangle = \frac{|01\rangle - |10\rangle}{\sqrt{2}} \quad \ldots\ldots(1.33)$$

The symbolization $|\beta_{00}\rangle, |\beta_{01}\rangle, |\beta_{10}\rangle, |\beta_{11}\rangle$ may be understood via the equation:

$$|\beta_{xy}\rangle \equiv \frac{|0, y\rangle + (-1)^{x}|1, y'\rangle}{\sqrt{2}} \quad \ldots\ldots(1.34)$$

where $\bar{y}$ is the negation of y.

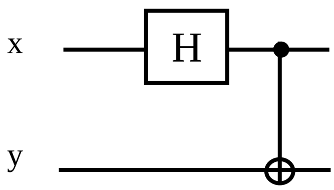

Fig. 1.5. Bell state creation circuit.

Table 1. 2. Bell states quantum circuit and truth table.

In	Out
$\|00\rangle$	$(\|00\rangle+\|11\rangle)/\sqrt{2}\equiv\|\beta_{00}\rangle$
$\|01\rangle$	$(\|01\rangle+\|10\rangle)/\sqrt{2}\equiv\|\beta_{01}\rangle$
$\|10\rangle$	$(\|00\rangle-\|11\rangle)/\sqrt{2}\equiv\|\beta_{10}\rangle$
$\|11\rangle$	$(\|01\rangle-\|10\rangle)/\sqrt{2}\equiv\|\beta_{11}\rangle$

1.11 Communication Protocols.

Quantum communication is a mechanism for transferring Quantum information between two parties efficiently and securely. Therefore, this field aroused the interest of researchers and scholars, and many practical experiments were conducted through which information was sent over a distance of up to 100 km through both free space and fiber [21-24]. Unfortunately, many problems occurs beyond this distance due to the photon loss in the channel and dark count produces by detectors [25]. To overcome such obstacle a quantum repeater protocol is introduced first by Briegle et al.[26]. Where, a combination of quantum memory and entanglement was used to extent the distance. The experimental implementation of quantum repeater (QR) still un verified until (2001) as Duan, Lukin, Cirac and Zoller (DLCZ) succeed in implementing QR based on linear optics and atomic ensembles [27]. Following DLCZ significant progress had been done in this field and many ideas and protocols are proposed such as (BB84) which was introduced by C. Bennett and G. Brassard in 1984 [28]. Afterward, numerous variations of the essential protocol have been produced [29].

- **Teleportation**

is a technique for transmitting an arbitrary quantum state from one position to another without any physical movement containing the state through the superseding space. This can be achieved with the assistance of a supplementary bipartite entangled state, one subsystem of which is near the state to be teleported, the other subsystem will hold the quantum state after the teleportation is complete, Figure (1.6) [30-31].

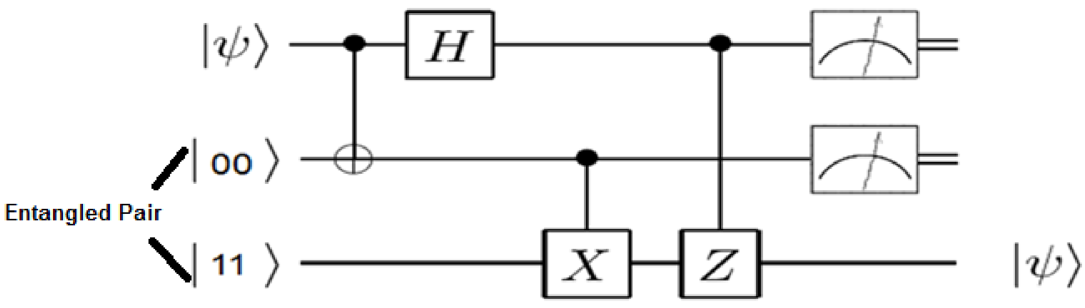

Fig. 1.6: Quantum teleportation scheme. A quantum state $|\psi\rangle$ transmitted from one location to another with assistance of CNOT gate, Hadamard gate H, entangled pair and Pauli transformation X and Z [31].

For instance: If "Alice and Bob" share an entangled state, and Alice (Bob) can transmit an unknown quantum state to Bob (Alice) without physically moving the unknown state through a process called quantum teleportation [4]. Suppose Alice holds the qubit state $|\Psi\rangle C = \alpha|0\rangle + \beta|1\rangle$, she and Bob share any Bell state $|\Psi\rangle AB$ (Choosing the Bell state $|\Phi+\rangle$ state for this example). The entire composite system is then termed by [32]:

$$|\varphi\rangle_{AB}|\varphi\rangle_{C} = |\Phi^{+}\rangle_{AB}(\alpha|0\rangle + \beta|1\rangle) \quad \ldots\ldots\ldots\ldots\ldots\ldots (1.35)$$

$$|\varphi\rangle_{ABC} = \frac{1}{\sqrt{2}}(|00\rangle + |11\rangle)(\alpha|0\rangle + \beta|1\rangle) \quad \ldots\ldots\ldots\ldots (1.36)$$

$$= \frac{1}{\sqrt{2}}(\alpha|000\rangle + \alpha|110\rangle + \beta|001\rangle + |111\rangle)\ldots \quad (1.37)$$

If Alice performs a BSM on the two $qubits$ in her possession, then conditional on Alice's measurement outcome Bob efficiently gets one of the following states:

$$\langle\Phi^{+}_{AC}|\varphi_{ABC}\rangle \rightarrow \alpha|0\rangle_{B} + \beta|1\rangle_{B} \quad \ldots\ldots\ldots\ldots\ldots (1.38)$$

$$\langle \Phi_{AC}^{-} | \varphi_{ABC} \rangle \rightarrow \alpha |0\rangle_B - \beta |1\rangle_B \quad \ldots\ldots\ldots\ldots\ldots\ldots (1.39)$$

$$\langle \Psi_{AC}^{+} | \varphi_{ABC} \rangle \rightarrow \beta |0\rangle_B + \alpha |1\rangle_B \quad \ldots\ldots\ldots\ldots\ldots\ldots (1.40)$$

$$\langle \Psi_{AC}^{-} | \varphi_{ABC} \rangle \rightarrow \beta |0\rangle_B - \alpha |1\rangle_B \quad \ldots\ldots\ldots\ldots\ldots\ldots (1.41)$$

Where each state occurs with a probability of 1/4. Depending on the measurement result of the BSM from Alice, Bob can apply a phase flip and/or a bit flip to correct his state, as characterized in (table 1.3) Bob then holds a state that is identical to $|\psi\rangle_C$ original held by Alice. So as to perform the teleportation, they proceed as follows [32]:

Alice performs a BSM between the *qubit* $|\psi\rangle_C$

andsubsystem A of the Bell state $|\psi\rangle_{AB}$.

$\Downarrow$

Alice sends her measurement outcome to Bob.

$\Downarrow$

Subsystem B collapses into one of the following states,
depending on the outcome of Alice's measurement

$\Downarrow$

Result	**State of system B**
$\lvert\Phi^+\rangle$	$\alpha\lvert 0\rangle + \beta\lvert 1\rangle$
$\lvert\Phi^-\rangle$	$\alpha\lvert 0\rangle - \beta\lvert 1\rangle$
$\lvert\Psi^+\rangle$	$\beta\lvert 0\rangle + \alpha\lvert 1\rangle$
$\lvert\Psi^-\rangle$	$\beta\lvert 0\rangle - \alpha\lvert 1\rangle$

Fig. 1.7: Quantum teleportation performing steps.

Depending on what Alice sends him, Bob sends system B through a unitary channel described by one of the following operators illustrated in table 1.3 as:

Table 1.3. Bob's correctional operation on his $qubit$, depending on the Bell state measurement outcome.

Bell state measurement outcome (Result)	Unitary	Bob's operation
$\|\Phi^+\rangle$	I	Do nothing
$\|\Phi^-\rangle$	Z	Phase flip
$\|\Psi^+\rangle$	X	Bit flip
$\|\Psi^-\rangle$	ZX	Bit and phase flip

Here X and Z are Pauli matrices. After this correction, system B ends up in the state $|\psi\rangle_B = \alpha|0\rangle + \beta|1\rangle$. Several properties of quantum teleportation are to be noted as [32].

1. Alice does not need to know what $|\boldsymbol{\psi}\rangle_{\mathbf{A}}$. In order to teleport it, all that is necessary is that she measure it jointly with one subsystem of a Bell State.
2. After the teleportation is finished . Alice only has a random Bell state; she no longer has a copy of $|\psi\rangle_A$.
3. Bob cannot construct $|\psi\rangle_B$ without receiving Alice's measurement result. Conversely, the information sent from Alice to Bob is, by itself, not sufficient to reconstruct the state $|\psi\rangle_A$.

- **Entanglement Swapping**

Entanglement swapping is a method used to connects EPR states shared between neighboring stations into a distant EPR state. The purpose of entanglement swapping is to create shared entanglement between the source and the destination nodes. Therefore, entanglement swapping may be imagined as a set of quantum teleportation steps or as “extended” teleportation protocol, which is able to bridge the large distances between distant stations. The details for two stations A and B and a repeater station between them are illustrated in Figure (1.8) [21].

Phase 1. Simultaneous entanglement generation between Station A and Repeater, and Repeater and Station B.

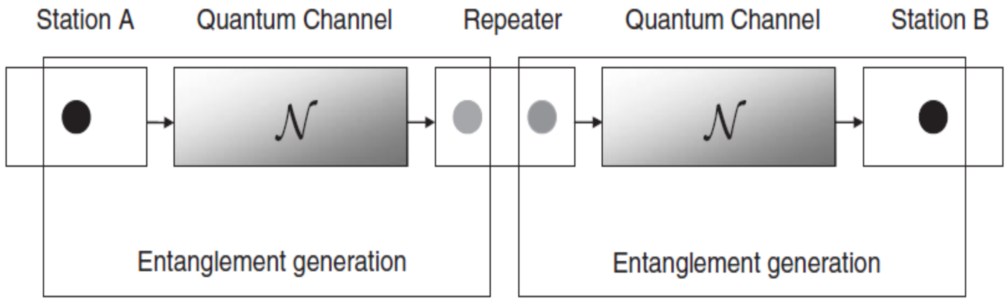

Phase 2. Qubits in the intermediate repeater are measured. The measurement results in 2 classical bits. The measured qubits are freed. The classical bits are sent to Stations A and B over the classical channel.

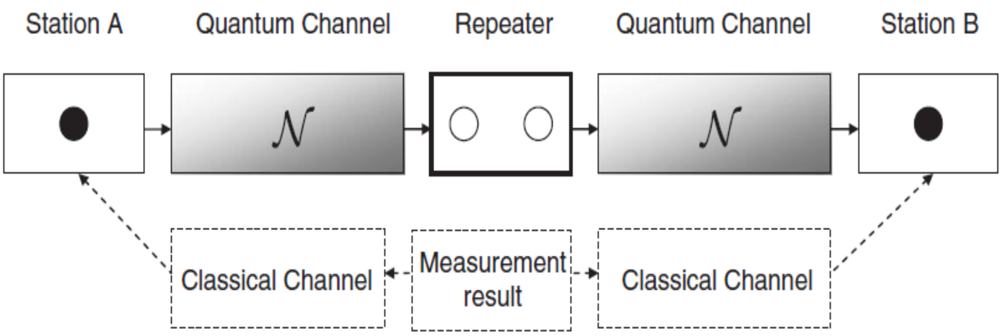

Phase 3. Swapped entanglement between Stations A and B.

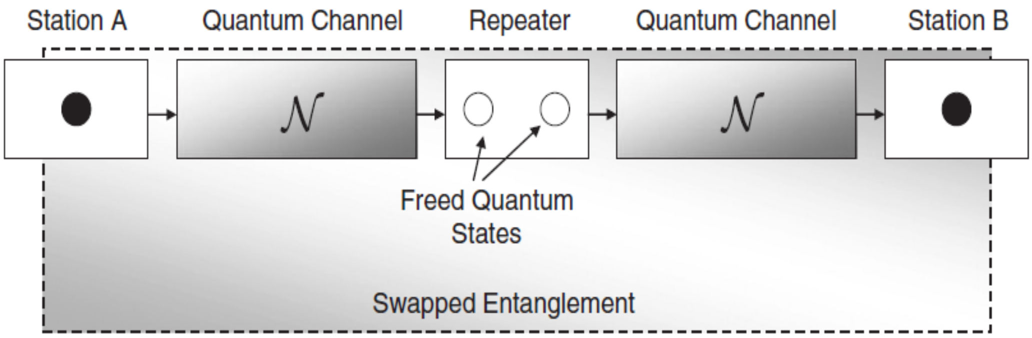

Fig. 1.8. Entanglement swapping. The transmission of entanglement from station A to station B, through a repeater. The transmission is based on shared and purified EPR states and classical communication, with local transformations.

1.12 Long Distance Quantum Communications

Long distance transmission of a quantum state is restricted by the exponential decay of the information because of the losses inherent in the communication channel. Correspondingly, the amplification of signals conveying quantum information is impossible due to no-cloning theorem. hence, to overcome such obstacle a quantum repeater is introduced [21].

1.13 Quantum repeater

According to the impossibility of transmitting quantum state between two parties due to the exponential transmission loss, an intermediate stations are equipped between the two parties. These stations are known as quantum repeater (QR), which is firstly proposed by In 1998, H. J.Briegel et al. [33] who suggested a quantum repeater protocol to generate entanglement between two distant parties by performing entanglement swapping, entanglement purification, and quantum memory [34,35].

The general principles of a QR are illustrated in Figure (1.9), in which the channel between two destinations is divided into many parts, each of these part known as node and entanglement is established between neighboring nodes. The entanglement between the closest sites could be established which expand the communication length by entanglement swapping. In real, entanglement swapping isn't flawless and the fidelity of entanglement will lessen altogether after a couple of association steps. Hence, entanglement purification [35,36] must be actualized to enhance the entangled pairs quality.

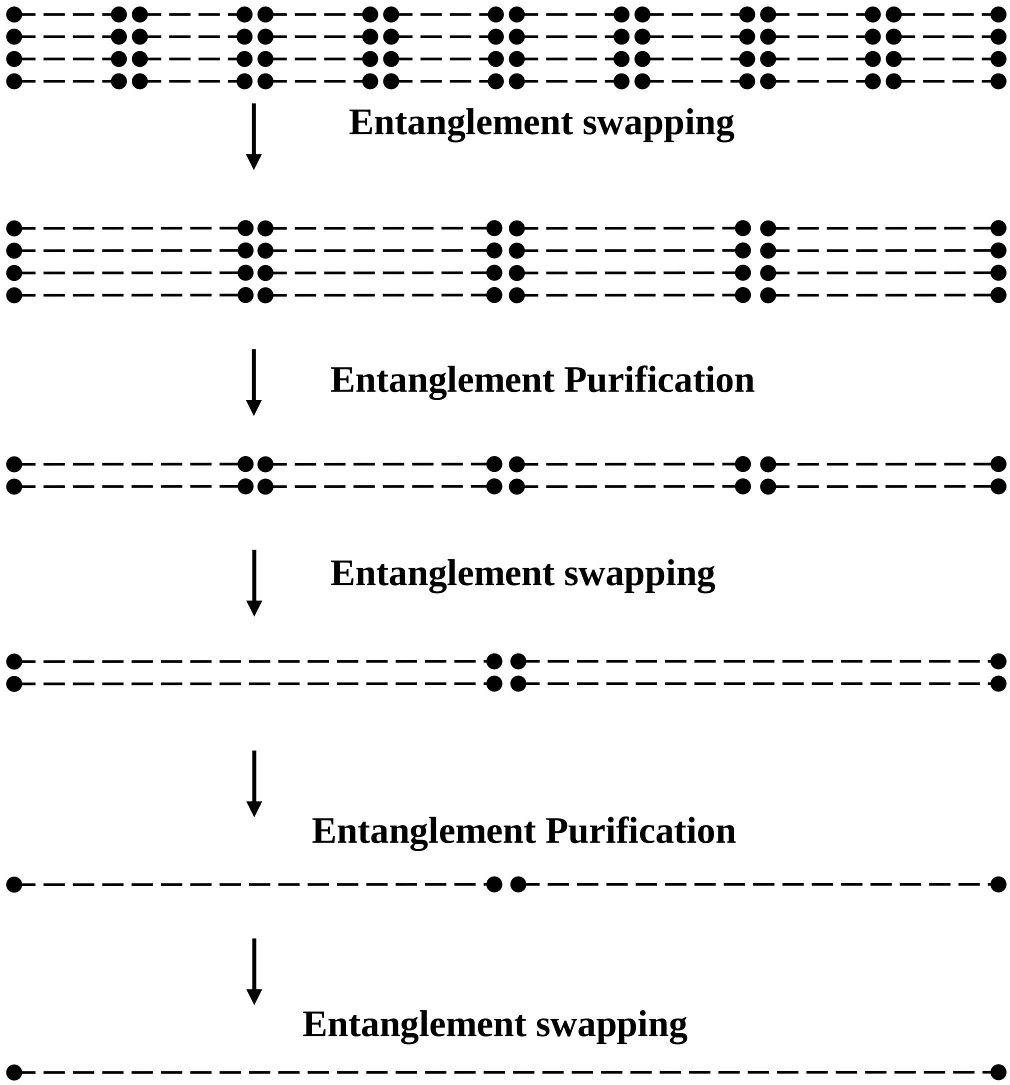

Fig. 1.9. QR protocol: entanglement swapping used to expand the communication channel, while entanglement purification is used to enhance the fidelity of the entangled pair [36].

As appears in figure (1.9), a nesting purification scheme is realized by doing entanglement swapping and entanglement purification many times until a remote entangled pair with high fidelity is established between the two parties. It was shown that time overhead and sources needed to establish the remote entangled pair are related polynomially to the distance [37].

Many quantum repeater schemes are proposed with different ideas, some of these are implemented practically and another just theoretical schemes. Most of the proposed quantum repeater schemes based on using optical fiber as transmission channel and an identical quantum memories in the nodes of quantum repeater [32,38-43] while other used non identical quantum memories [44]. Also many schemes based on a free space as transmission channel [45-50].

As a basic requirement, a QR transfers data at a rate (in bits per mode per channel use) exceeding the quantum capacity of a total channel. The essential ideas for most QR schemes are to divide a general channel into N smaller channel stations. The principal upper bound on the quantum communication limit of a lossy channel scales straightly with transmissivity η, which represents the ratio of the amplitudes of the electromagnetic radiation that goes through the chnnel. Isolating the channel into N smaller parts will empower the key rate to scale as $\eta^{1/N}$, as photons will encounter loss just in a small amount of the total channel. Clearly, an extra assistant devices called nodes are needed between channel stations for the QR to work as proposed. For most QR, each node comprises of two quantum memories. The framework will use an entanglement swapping scheme at every node, which connects the links together [51].

1.13.1 Quantum Memories

Quantum memory (QM) is an important part for any QR for the implementation of quantum communication for long-distances. In the QR protocol [52], the communication channel is divided into many links with lengths comparable with communication channel attenuation length L_{att}. Entanglement is then produced and purified for each link before it is distributed over a longer distance by an entanglement swapping process. Consequently, a teleportation of quantum data can be achieved. Due to the probabilistic nature of the purification [53] and the need of storing the already successful states in QM while waiting for others, quantum memory with long storage time is vital to accomplish scalable quantum communication systems [54].

Among different proposed QR schemes, the DLCZ protocol has attracted in much consideration by experimentalists [28]. This protocol depends on the entanglement between single photons and aggregate excitations in atomic ensembles. Following this fundamental work, the critical advance has been made as of late. Non classical correlation between the light generated in the aggregate emission from an atomic ensemble and the retrieved aggregate excitation has been beheld [55, 56]. Measurement-induced entanglement has additionally been created between two atomic ensembles. Recently, entanglement-based quantum teleportation and entanglement swapping with an built-in quantum memory have been shown between photonic and atomic qbits [57, 58].

Different types of QMs have been proposed and implemented, such as atoms in optical cavities [59], trapped atoms [60], nitrogen-vacancy centers [61], and atomic ensembles [62], Trapped ions have been exhibited to have decoherence times on the scale of seconds [63, 64], while the coupling efficiency of the emitted photons into fiber for this system is low of around 0.03%-0.05% [65, 66]. However, the coupling efficiencies of optical cavities are over 30% [67]. Bell state measurements can be performed between neighboring particles deterministically [68] or by optically perusing out and entangling photonic states [51].

1.13.1.1 Types of Quantum Memories

The variety of quantum memory candidates fall roughly into two categories, according to whether they rely on single quantum emitters or large ensembles of particles. They further differ in both the physical substrate onto which quantum information is mapped and the protocol used to realize this mapping.

Among the quantum memories based in single quanta one can find [55,58]:

1. Single atoms in cavities. Optically trapped single atoms in cavities have been used to demonstrate the storage of polarization qubits and the generation of matter-matter entanglement between remote places. The best reported qubit storage showed an efficiency of $\eta = 9\%$, a fidelity of 93% and a decay time of $\tau = 180\ \mu s$.

2. Individual trapped ions. Electrically trapped ions in vacuum chambers are well controlled and individually adressable single quantum systems. Their applications to quantum networks have been reviewed in and. They have been shown to exhibit long coherence times. Recent achievements with these systems include the quantum teleportation of a qubit between remote ions and the mapping of a single-photon polarization state onto a single ion. In this last experiment, the storage fidelity was 95% and the low efficiency (below 1%) was compensated by a heralding mechanism. Muller and Eschner have proposed to use single 40Ca+ ions as a substrate for the storage of a polarization qubit a t $\lambda = 854$ nm.

3. Nitrogen-vacancy centers in diamond. Nitrogen-vacancy centers (NVC) are naturally occurring or engineered defects in bulk diamond exhibiting rich quantum properties. Entanglement between a single photon and the electronic spin of a NVC has been demonstrated as well as the transfer of the electronic state of the NVC to its nuclear spin which has a much larger coherence time, on the order of the millisecond.

Ensemble-based quantum memories are more versatile as their intrinsic multimode nature gives them the capacity to store not only “regular” (polarization) qubits but also various types of continuous variable quantum states such squeezed states or even Schrodinger cats. They also support a variety of different memory protocols. So far, they include [62, 68]:

1. Cold or ultra-cold atomic gases, which are the earliest media used for light storage. Very pure gases of alkali atoms are prepared via laser cooling at various temperatures, from a few millikelvins in magneto-optical traps to microkelvins in dipole traps and even in the nanokelvin range in Bose-Einstein condensates (BEC). Once cooled and trapped, cold atoms can be used to implement various memory protocols. The first one ever demontrated relied on Electromagnetically Induced Transparency (EIT) and the associated ultraslow light effect. While being the oldest memory protocol, it has very promising features and is therefore still the subject of intense reserach. In particular, it is the one we will use in the rest of this thesis. Cold atomic ensembles in off-resonant EIT (Raman) conditions are also the medium of choice for the implementation of the DLCZ protocol.

2. Warm atomic vapors. Hot gases support memory protocols that are very similar to the ones implemented in cold atomic ensembles (six orders of magnitude in temperature put aside). EIT based light storage was demonstrated in them almost at the same time as in cold atoms. They have been used in several EIT or Raman-based optical storage experiments (some of which exhibited a quantum behavior in GEM experiments or in Faraday-interaction-based memory experiments.

3. Rare earth doped crystals. These materials can experience extremely long coherence times at cryogenic temperatures. They are therefore studied as versatile light storage media. Following the demonstrations of EIT-based light storage in atomic gases, a similar experiment was performed in a crystal. In addition to EIT, crystals are also well suited for photon echo protocols such as the Controlled Reversible Inhomogeneous Broadening (CRIB) an equivalent of the Gradient Echo Memory or its discrete version, the Atomic Frequency Comb (AFC).

1.14 Optical Fiber

Optical fiber is used in telecommunications to transmit telephone signals, Internet communication, quantum communications, and cable television signals. It is also used in other applications, such as medical, government, defense, industrial and commercial. In addition to serving the purposes of telecommunications, it is used as light guides, for imaging tools, lasers, hydrophones for seismic waves, SONAR, and as sensors for measuring pressure and temperature.

The most important advantage of the recently developed quantum security structures is that, they can be easily implemented with the current optical network. The standard optical fibers may be combined to create a universal quantum communication networks. Quantum cryptographic is one of the most important protocols in the field of quantum information processing. Optical fibers have an essential role in quantum cryptography, as the data is encoded in the photons polarization states. In quantum cryptography, also, as the sender and receiver in quantum cryptography will communicate through macroscopic distances, then optical fiber becomes practical choice to propagate and preserve the photonic qubits physical properties. Also, in the case of quantum key distribution optical fiber is a practical choice to communicates the parts of these systems [69].

The most important factor in any communication system is the losses of the optical signals that are transmitted through the optical fiber [70]. The minimum loss in fused silica, which is around 1550 nm is slightly less than 0.2 dB/km as it is shown in Figure (1.10). This limit is important, since it sets the amplifier spacing in communications systems, and thus is a major cost of a transmission system [71].

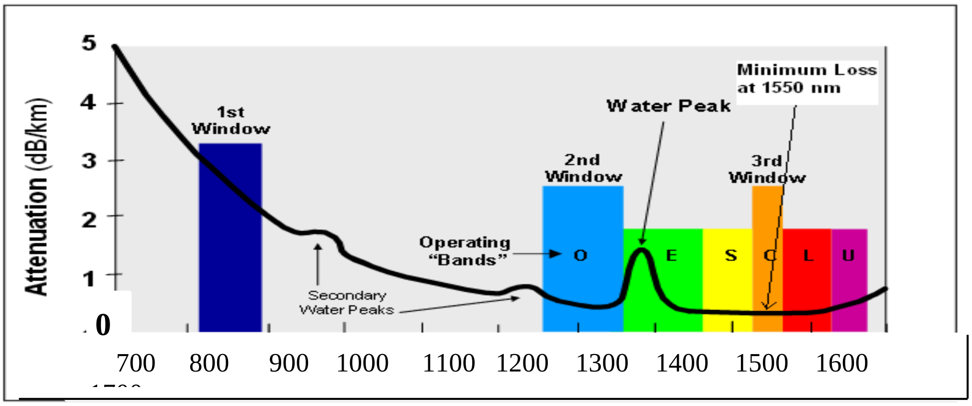

Fig. 1.10 Attenuation spectrum of optical fiber [71].

1.14.1 Dispersion

In telecommunication systems, information is transmitted as binary data, taking the form of light pulses in optical fibers. In the field of optical waveguides, dispersion is a generic term referring to all phenomena causing these pulses to spread while propagating and they eventually overlap and light pulses could not be distinguished by the receiver [72]. There are essentially three causes of dispersion.

1.14.1.1 Chromatic Dispersion

Chromatic intramodal dispersion is an important phenomenon in the propagation of short pulses in optical fibers. Temporally short pulses have a large spectral bandwidth. The different spectral components of the pulse travel through the medium at slightly different group velocities because of chromatic dispersion, which can result in a temporal broadening of the light pulses with no effect on their spectral compositions. This phenomenon is referred to as group velocity dispersion (GVD), [72].

1.14.1.1.1 Material Dispersion

Material dispersion is an important effect because when a short pulse propagates through an optical fiber its width gets broaden. The effects arise from the variation of the refractive index of the material as a function of wavelength. This causes a wavelength dependence of the group velocity of any given mode, that is, pulse spreading occurs even when different wavelengths follow the same path [72].This phenomena can be understood by expanding the mode-propagation constant β in a Taylor series about the frequency $w_o$at which the pulse spectrum is centered, [73]

$$\beta(\omega) = n_{eff}(\omega)\frac{\omega}{c} = \beta_o + (\omega-\omega_o)\beta_1 + \frac{1}{2}(\omega-\omega_o)^2\beta^2 + \frac{1}{6}(\omega-\omega_o)^3\beta^3 + \ldots \quad \ldots\ldots\ldots (1.42)$$

where:

$$\beta_m = \left(\frac{d^m\beta}{d\omega^m}\right)_{\omega=\omega_o} \quad (m=1,2,\ldots) \quad \ldots\ldots\ldots\ldots\ldots\ldots (1.43)$$

$$\beta_o = n_{eff}(\omega_o)\frac{\omega_o}{c} \quad \ldots\ldots\ldots\ldots\ldots\ldots(1.44)$$

$$\beta_1 = \frac{1}{c}(neff + \omega \frac{dn_{eff}}{d\omega}) = \frac{1}{\upsilon_g} = \frac{n_g}{c} \quad \text{.................. (1.45)}$$

$$\beta_2 = \frac{1}{c}(2\frac{dn_{eff}}{d\omega} + \omega \frac{d^2 n_{eff}}{d\omega^2}) = \frac{d}{d\omega}(\frac{1}{\upsilon_g}) \quad \text{................ (1.46)}$$

where β_o is the mode-propagation constant of frequency ω_o, v_g is the group velocity, and n_g is the group index.

The group velocity is the speed of the envelope of an optical pulse propagating in a fiber. The coefficient β_2 determines the changes in the group velocity of an optical pulse as a function of optical frequency. This phenomenon is known as group velocity dispersion (GVD) and is responsible for pulse broadening. Thus, β_2 is called the GVD parameter. In general, we must retain terms up to the second-order dispersion β_2 to describe pulse propagation in dispersive media, and for ultrashort pulses or those with a wide frequency spectrum it may sometimes be necessary to also include higher order terms.

The dispersion parameter D is commonly used in place of β_2 to describe the total dispersion of a single mode fiber. It is related to β_2 by the relation

$$D \cong \frac{d\beta_1}{d\lambda} = -\frac{2\pi}{\lambda^2}\beta_2 \quad \text{............................ (1.47)}$$

And is expressed in unit of ps/(km.nm).

Since GVD mainly comes from the combined effects of material and waveguide dispersion, D can be written as the sum of two terms, as [74]:

$$D_{intra} = D_M + D_W \quad \text{................................ (1.48)}$$

where D_M is the material dispersion and D_W is the waveguide dispersion.

$$D_M = \frac{-\lambda}{c}\frac{d^2 n_{eff}}{d\lambda^2} \quad \ldots\ldots\ldots\ldots\ldots\ldots\ldots \quad (1.49)$$

where n_{eff} is the effective refractive index given by [44]

$$n_{eff} = \sqrt{fn_{air}2 + (1-f)n_{silica}2} \quad \ldots\ldots\ldots\ldots .\ (1.50)$$

where f is the air filling fraction**,** n_{air} obtained from the following equation [75]:

$$n_{air} = 1 + 0.0472326(173.3 - \frac{1}{\lambda^2})^{-1} \quad \ldots\ldots\ (1.51)$$

But When the holes of the hollow core photonic crystal bandgap fiber filled with materials other than air specially the n_{air} in equation (1.51) replaced by n_m that obtained by the following Cauchy formula [76]

$$n_m = ac + \frac{bc}{\lambda^2} + \frac{cc}{\lambda^4} \quad \ldots\ldots\ldots\ldots\ldots\ldots\ldots\ (1.52)$$

where ac, bc, cc are the Cauchy coefficients and n_{silica} in equation (1.17) is the refractive index of silica that get from the following Sellmeier equation[77]:

$$n_{silica}(\omega) = 1 + \sum_{j=1}^{m}\frac{B_{sj}\omega_j^2}{\omega_{sj}^2 - \omega^2} \quad \ldots\ldots\ldots\ldots\ldots\ldots..\ (1.53)$$

where ω_{sj} the resonance frequency and B_{sj} is the strength of j_{th} resonance. In the case of bulk-fused silica, these parameters are obtained empirically with m = 3 to the measured refractive index, and they are found to be:

B_{s1} = 0.6961663 , B_{s2} = 0.4079426
B_{s3} = 0.8974794 , λ_1 = 0.0684043 μm
λ_2 = 0.1162414 μm , λ_3 = 9:896161 μm

where $\lambda_j = \frac{2\pi c}{\omega_{sj}}$ [48].

1.14.1.1.2 Waveguide Dispersion

The group velocity of guided optical pulses depends on the wavelength even if material dispersion is negligible. This dependence is known as the waveguide dispersion [77]. The contribution of waveguide dispersion D_W to the dispersion parameter D is given by the equation (1.51). D_W depends on the difference in the index Δ which was given by the following equation (1.54):

$$\Delta = (n_{co} - n_{cl}) / n_{co} \quad \ldots\ldots\ldots\ldots\ldots\ldots\ldots\ldots (1.54)$$

1.14.1.2 Intermodal Dispersion

It results from the propagation delay differences between modes within a multimode fiber. As the different modes that constitute a pulse in a multimode fiber travel along the channel at different group velocities, the pulse width (D) at the output is dependent upon the transmission time of the lowest and fastest modes as expressed by (1.55) [72]:

$$D^2_{total} = (D_{material} + D_{waveguide})^2 \, \Delta \, \lambda^2 + D^2_{modal} \ldots\ldots (1.55)$$

1.14.1.3 Polarization Mode Dispersion

A fundamental property of an optical signal is its polarization state. Polarization refers to the electric-field orientation of a light signal, which can vary significantly along the length of a fiber. As shown in Figure (1.11), signal energy at a given wavelength occupies two orthogonal polarization modes. A varying birefringence along its length will cause each polarization mode to travel at a slightly different velocity and the polarization orientation will rotate with distance. The resulting different in propagation modes will result in pulse spreading that called polarization mode dispersion (PMD) [78].

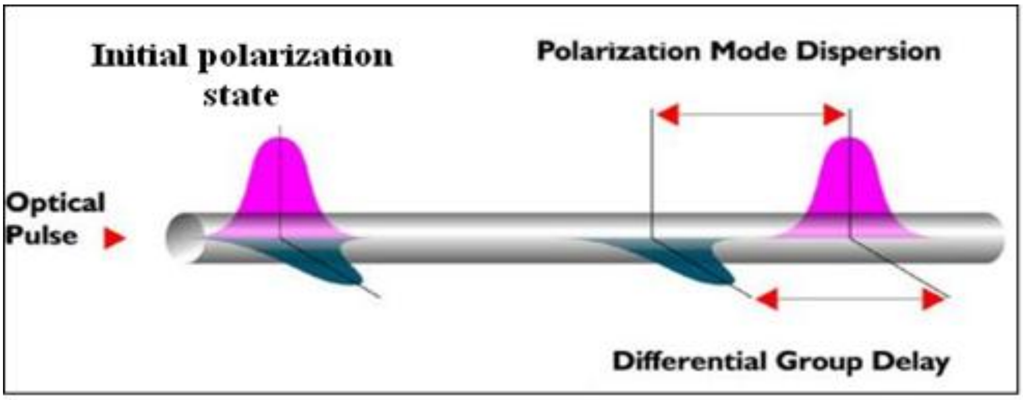

Fig. 1.11 Variation in polarization states of an optical pulse at it passes through a fiber [78].

1.15 Classical Quantum Interface

The personality of classical and quantum information is essentially different. There are numerous facts in quantum frameworks that can't be described classically, like entanglement, which makes it conceivable to store quantum information in the correlation of quantum states. Entangled quantum states are called EPR states after Einstein, Podolsky and Rosen, or Bell states, after J. Chime.

Quantum computing objectives is to solve difficult issues through devices dependent on quantum mechanical standards. but, human organs match the classical world in this manner we need interfaces between the client and the tools. The interface at the yield is liable for how to change the quantum state of the framework into classical states, It is called measurements which is an irreversible activity, annihilating quantum information and exchanging it by classical one [79].

The transmission of product states can be defined like classical information, then again, the properties of quantum entanglement can't be implemented by the components of classical information theory. Obviously, the components of classical information theory can be seen as a subset of the bigger and more mind boggling quantum information theory. The connection among quantum and classical information theory is represented in figure (1.12) [21].

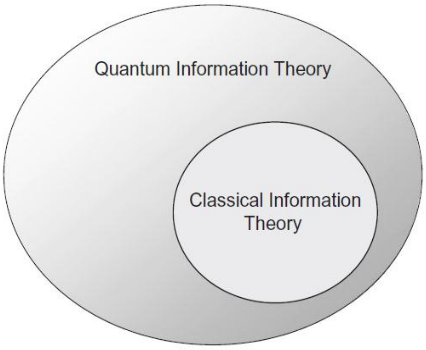

Fig. 1.12. The elements of classical information theory can be viewed as a subset of quantum information theory.

The today building blocks of quantum processors are advanced enough to begin work on scaling these systems into complex quantum machines. The main subsystem of all quantum machines is the interface between the isolated qubits that encode quantum information and the classical control and reading technology needed to operate them. As a few qubit-containing devices are combined to create larger, fault-tolerant quantum systems in the near future, the classical quantum interface will present new challenges that increasingly require approaches from engineering disciplines along with ongoing fundamental developments in materials, physics, and mathematics [80].

A conceivable structure for the quantum-classical interface which can be used to control and read out quantum technology is illustrated in figure (1.13). In which information is passed to and from qubits in the quantum physical layer by classical circuits like digital-to-analogue converters (DACs), analogue-to-digital converters (ADCs), arbitrary waveform generators (AWGs), amplifiers (Amps) and multiplexers (MUXs). Application specific integrated circuits (ASICs) or field-programmable gate arrays (FPGAs) implement high-speed logic and feedback between readout and control [81].

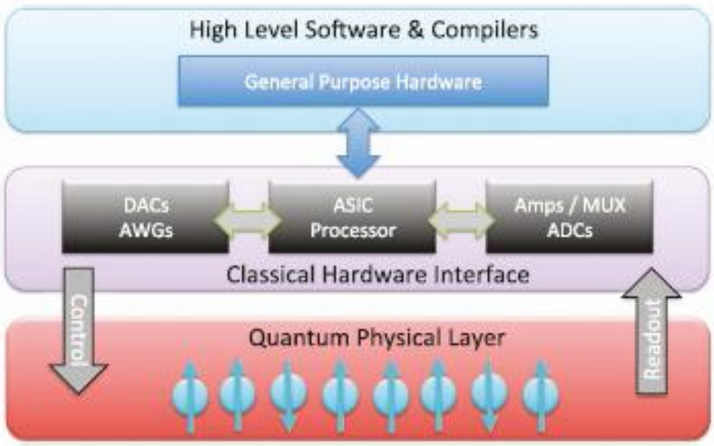

Fig. 1.13 Quantum-classical interface for controlling and reading out quantum technology[74].

future communications systems will represented by the combination of quantum communication systems and classical systems utilizing the components of classical data processing (figure 1.14). The huge utilization of optical fiber and latent optical components permits us to utilize quantum cryptography. Therefore, to spread quantum cryptography, interfaces should be executed that can manage together both classical and quantum channels. These classical parts will be incorporated into the less basic pieces of the protocols, subsequently these arrangements won't diminish the degree of security. The present carried out useful quantum networks all contain some classical components, and cannot be eliminated in future [10].

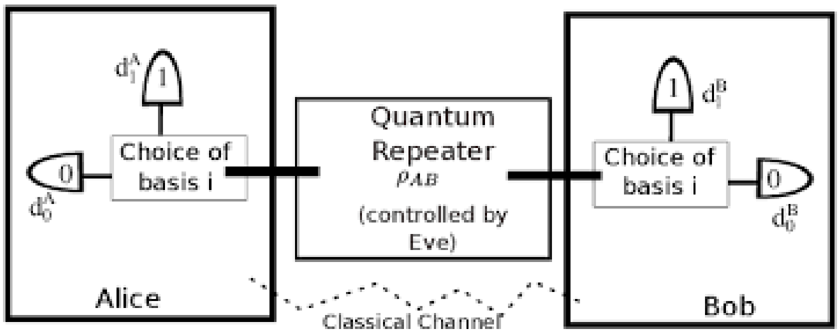

Fig. 1.14. Combination of quantum and classical channel in communication network [10].

Quantum computer also requires a classical controller to control and peruse out qubit states (figure 1.15). Whereas classical controller and quantum processor should be put in closeness, in light of the requirement for actual interconnections between them. This prerequisite will be particularly tough when the quantity of qubits, and subsequently the wires associating them, will develop to extremely huge numbers. Since most quantum processors these days require activity at profound cryogenic temperature well under 1 K [80].

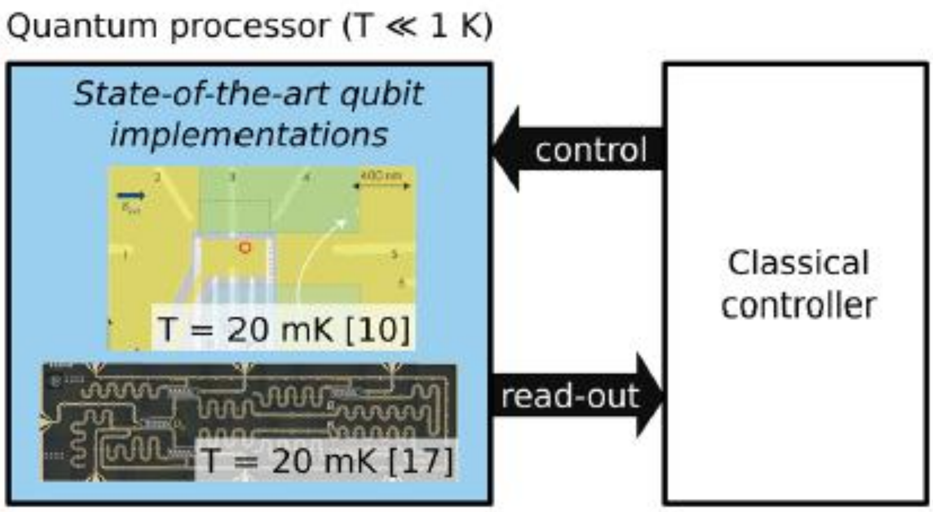

Fig. 1.15. Quantum classical interface in quantum processor[82]

1.16 Hybrid Network

Despite the fact that utilizing optical fiber made simple to utilize the optical light that contains the higher bandwidth and higher data than microwave channel, the latter has been utilized in the old style interchanges. Notwithstanding, all optical systems build up the delay factor [83], which is one of the primary elements should have been improved in 5G associations and beyond.

This compromisation is important to be concentrated so as the interest against the two systems turns out to be progressively authentic. Offering a straight forward territory that mounts the optical fiber isn't generally accessible because of the trouble of introducing the fiber that requires claimed or leased territories. In any case, much of the time, governments make simple this setting to be finished. All things considered, the expense of introducing the optical links for huge separations increments straightly with the covered zone. Nonetheless, this issue is just substantial for zones that are at. If there should arise an occurrence of variation in the landscape, the instance of deploying all quantum networks gets obstinate. Consequently, adjusting quantum and classical styles of communications turns to an arrangement, as appeared in Figure 1.16 [84].

Because the traditional style of communications that is its configuration spoke to by cloud system or conventional BS are predominately concentrated in the writing [85], this work focuses upon the hybrid and all quantum systems.

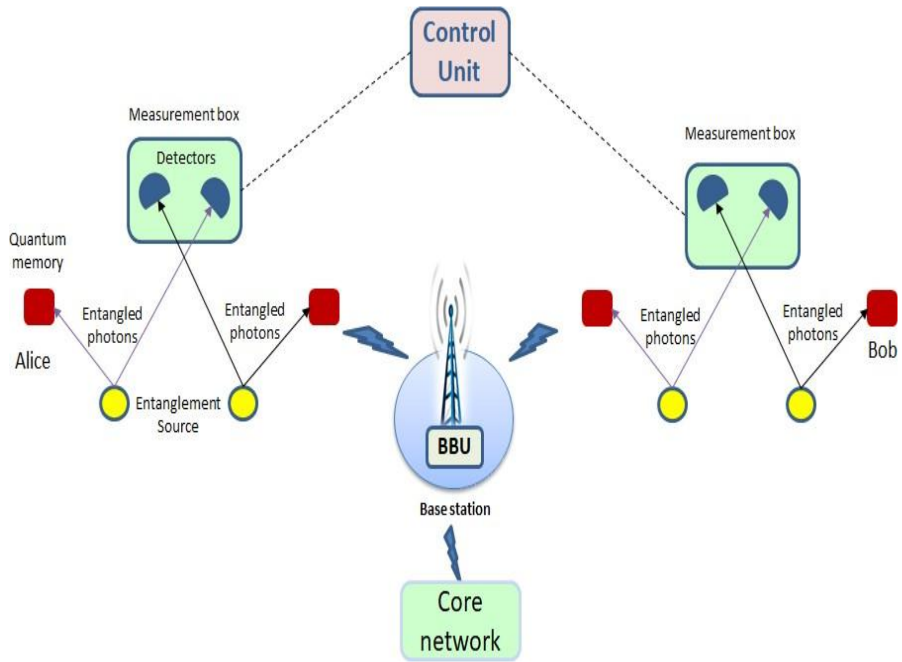

Fig. 1.16 The paradigm of quantum-classical networks [84].

Hybrid implies part of the channel has been supplanted by utilizing traditional BS that is topographically generally installed. Subsequently. this work has demonstrated the utilization of power, cost, information rate and the received energy effectiveness of both systems hybrid and quantum. Note that traditional communications is done at the time when the network subscribers connect wirelessly to the antenna of the BS, after, the base station transfers the users' data to the core network, generally called evolved packet core using an optical or wireless link. The evolved packet core contains several network units, generally packet gateway, serving gate way and mobility management entity. Each of these units performs many important and concatenated functions that help to maintain the subscribers' authenticity, connectivity, security, and provides the needed quality of service. The latter means that each user will be allocated specific amount of bandwidth so as its required data rate will be satisfied.

1.17 Aim of the Study

This Study aims to examine the effect of both decoherence time T_2 and coupling efficiency of the quantum memory on the performance of quantum repeater through using different types of quantum memories with different characteristics.

1.18 Literature Survey

In this section some of the studies proposed by preachers that are related to the present study are presented.

1. Luong D. (2015). The Practical Realization of Quantum Repeaters: An Exploration [40].

In this study, The analyses involve modeling the experimental imperfections due to various components of a quantum repeater, then calculate various quantities of interest. Also, in this study the entanglement phenomena is done through three methods to entangle two atoms: (1) interacting a coherent pulse with each atom, then performing an entangling measurement on the pulses; (2) interacting a single coherent pulse with each atom sequentially; (3) emitting an entangled photon from one atom and interacting it with the other atom. The success probability of each method is compared, as well as the quality of the entangled states produced by each one, taking into account imperfections which appear in a specific experimental implementation of such memories. The results of the study shows that there is a tradeoff between success probability and entangled state quality when coherent states are used, and that method 3 provides higher-quality entangled states than is possible with the other two methods.

2. Mastromattei Ch. (2017). Assessing the Practicality of a Simple Multi-node Quantum Repeater [32].

In this study a theoretical performance of a realistic multi-node quantum repeater that is implementable with current technology is assessed. A simple, one-way, multi-node quantum repeater that utilizes entanglement swapping in the absence of any quantum error correction or entanglement purification is introduced. The theoretical model of the quantum repeater, incorporating the imperfections of each component within the system is created. to get an accurate key rate using current, viable state of the art experimental parameters. Our main goal is to benchmark the performance of this specific multi-node quantum repeater. We compare the performance of this multimode system to that of a single node repeater, which has been previously analyzed for this architecture. We are interested to see if there is an advantage for introducing more nodes in this type of system. We also provide some suggestions for improving the key rate performance.

3. Wijdan M. K & Jawad A.K (2018). Quantum Repeaters Based on Multiplexed Single-Photon Source [39].

In this study, an efficient architecture for quantum repeaters based on multiplexing single-photon sources in combination with multiplexing multimode quantum memories was suggested to increase the entanglement between arbitrary photon number of remote quantum memories. The results illustrates that, there is improvement in the entire entanglement distribution rate. In this work, a simulation study was carried out using the Python 3.7 simulation software.

4. Adnan N. et al., (2020). Implementation of quantum repeater scheme based on non-identical quantum memories [44].

In this study, a multi-node sequential quantum repeater QR of a non-identical QMs is presented to interplay between the total channel efficiency and decoherence time T_2 of the quantum memories to enhance the execution of the quantum repeater (QR). The results show that the interplay between the decoherence time and efficiency in non-identical QR improves the key rate as compared to that of the identical QR, the distance of the channel can be extended by using non-identical QMs repeater scheme since quantum bit error rate is decreased, and the cost of fabricating non-identical QMs repeater is reduced since we use most QMs with low life time.

5. Johannes B., Hannes P., Tim S., Mikhail D. Lukin, Peter L., Anders S (2020). One-way quantum repeater based on near-deterministic photon-emitter interfaces [41].

A novel one-way quantum repeater architecture based on photonic tree-cluster states is proposed. Encoding a qubit in a photonic tree-cluster protects the information from transmission loss and enables long-range quantum communication through a chain of repeater stations. As opposed to conventional approaches that are limited by the two-way communication time, the overall transmission rate of the current quantum repeater protocol is determined by the local processing time enabling very high communication rates. Also, the results show that such a repeater can be constructed with as little as two stationary qubits and one quantum emitter per repeater station, which significantly increases the experimental feasibility.

6. Carlo Liorni, Hermann Kampermann & Dagmar Bruß (2021). Quantum repeaters in space [47].

In this study, a combine these two ingredients, quantum repeaters and satellite-based links, into a scheme that allows to achieve entanglement distribution over global distances with a small number of intermediate untrusted nodes is proposed. The entanglement sources, placed on satellites, send quantum states encoded in photons towards orbiting quantum repeater stations, where entanglement swapping is performed. The performance of this repeater chain is assessed in terms of the secret key rate achievable by the BBM92 cryptographic protocol. The results show that our scheme, even though more technically demanding, is superior in many situations of interest in comparison with other repeater chain architectures.

Chapter Two

Repeater Analysis & Methodology

This chapter will contain two topics, in the first one a brief description of the parameters of quantum repeater will be introduced. While in the second topic the methodology of the study will be presented. The flow chart of the structure of the study will be as shown in Fig. 2.1.

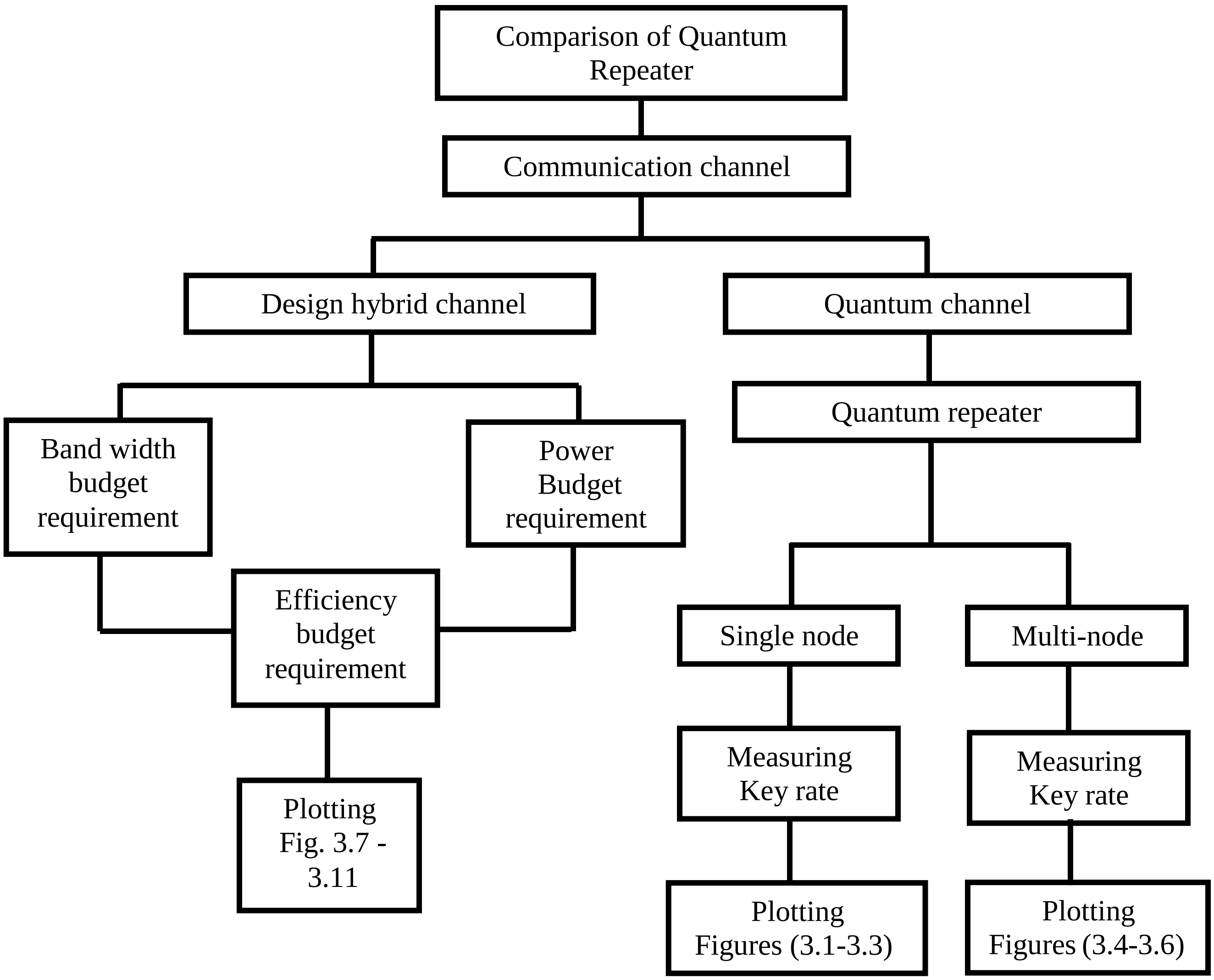

Fig 2.1: Structure of work

2.1. Description of Quantum Repeater Parts

As cleared in chapter one, the aim of any quantum repeater is to extend the distance that quantum state can reach though optical fiber or free space and overcome the exponential decay of the quantum state in the direct transmission case by distributing the entangled photon obtained from any laser source through the quantum repeater components which are illustrated in (Fig. 2.2).

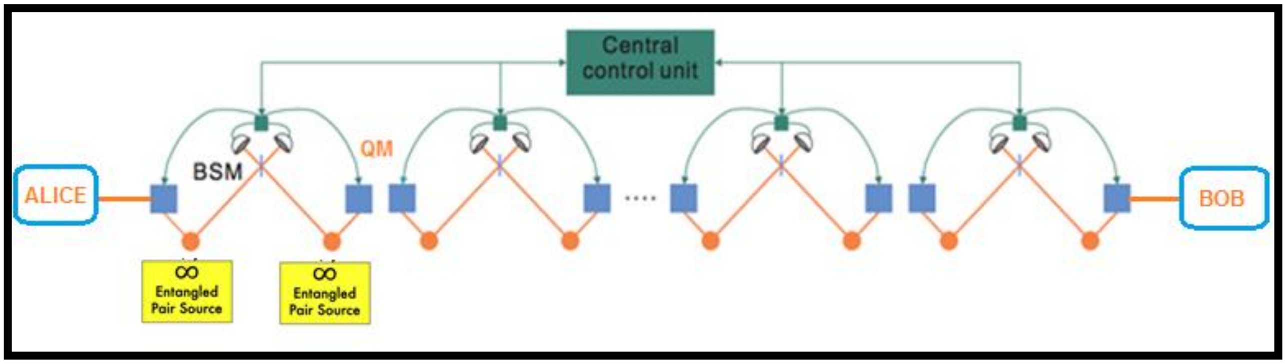

Fig. 2.2. Quantum Repeater

The schematic diagram shown in (Fig. 2.1) represent a multi node quantum repeater. Each node consist of two quantum memories located at each end of the node, two entangled photon sources, a Bell state measurement is performed between the two quantum memories, a central unit to control the operation steps of quantum repeater and some other parameters. In the following paragraphs a brief description of the important point of each part will be introduced..

2.1.1 Quantum Memories

The aim of the quantum memories in quantum repeater schemes is to store the quantum state for a specific time known as decoherence time T_2, then emit the entangled memory quantum state, that assumed to share a maximally entangled bipartite state, with a coupling efficiency η_p, and a preparation time T_{prep}.

The important parameters of each quantum memory that affected the performance of quantum repeater are the decoherence time and the coupling efficiency, these parameters are related inversely to each other as shown in (Fig. 2.3) [82,86].

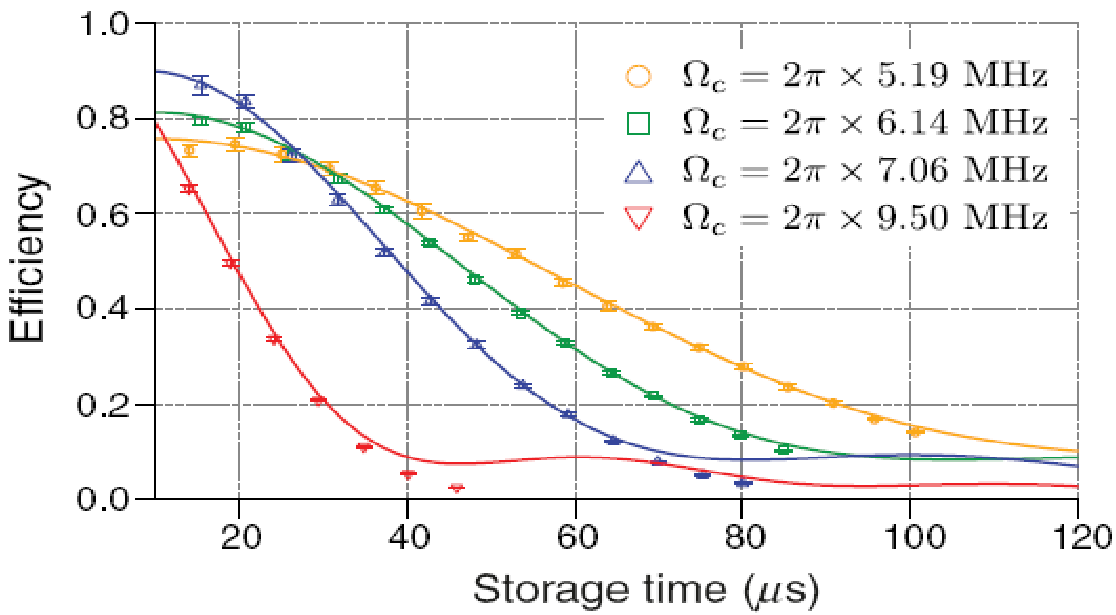

Fig. 2.3. Relation between quantum memory decoherence time and coupling efficiency.

2.1.2 Channels

The channel linked Alice and Bob is divided into three parts ($\mathbf{L_a}$, $\mathbf{L_{in}}$, and $\mathbf{L_b}$) where L_a represent the distance between Alice and the first quantum memory, $\mathbf{L_{in}}$ represents the inner links between quantum memories while $\mathbf{L_b}$

represent the distance from last quantum memories to Bob and as shown in (Fig. 2.4).

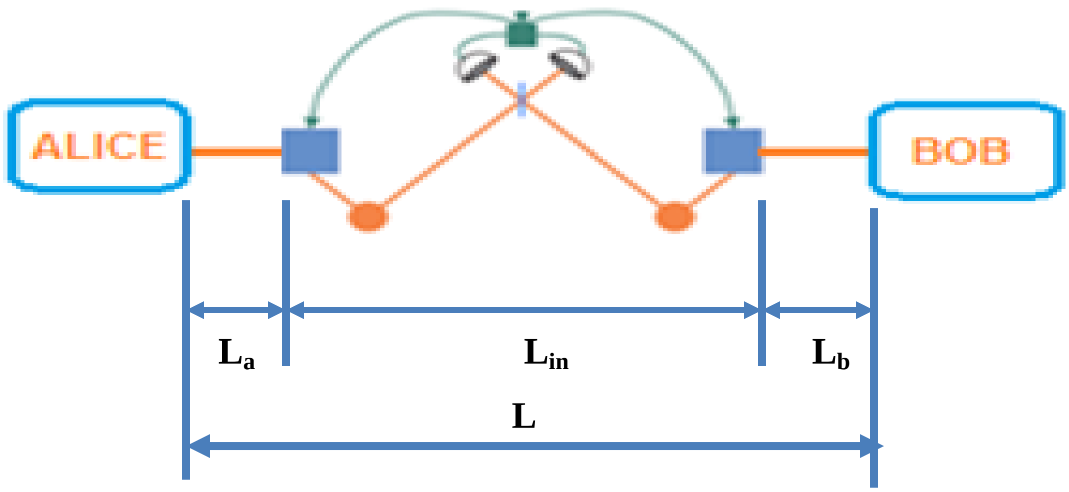

Fig. 2.4 Quantum repeater channel

The values of each distance can be calculated from the following equations [17].

The inner length ($\mathbf{L_{in}}$) segments can be expresses as:

$$L_{in} = \frac{(1 - x - y)}{(n - 1)} L \quad \text{……………..(2.1)}$$

While, the outer links are

$$L_a = xL \quad \text{and} \quad L_a = yL \quad \text{…………..….(2.2)}$$

Where x and y are spacing parameters.

The physical channel for most proposed quantum repeater schemes is optical fiber. The transmission efficiency (η_{ch}) of quantum state in optical fiber decreases exponentially with accordance of the fiber length as illustrated in the following equation [17].

$$\eta_{ch}(L) = \eta_{tot} e^{-L/L_{att}} \qquad \ldots\ldots\ldots\ldots..(2.3)$$

Where,

L_{att} is the optical fiber attenuation length and its equal to about 22km at 1550 nm wavelength.

η_{tot} is the channel total efficiency and equal to:

$$\eta_{tot} = \eta_p \eta_c \eta_\lambda \eta_d \qquad \ldots\ldots\ldots\ldots(2.4)$$

In which,

η_p : preparation efficiency

η_c : coupling efficiency

η_λ : conversion efficiency

η_d : detector efficiency

2.1.3 Entangled Photon Source

The operation of quantum repeater based on the distribution of a pair of entangled photons across the nodes of quantum repeater until Alice and Bob become entangled. The source of these entangled photon is obtained from a nonlinear optical process, in which a high energy photon obtained from laser source known as pump photon is transformed to a pair of low energy single photons called the signal and idler photons in a process called spontaneous parametric down-conversion **(**SPDC**),** or sometimes called parametric scattering or parametric fluorescence as shown in (Fig. 2.5) [87].

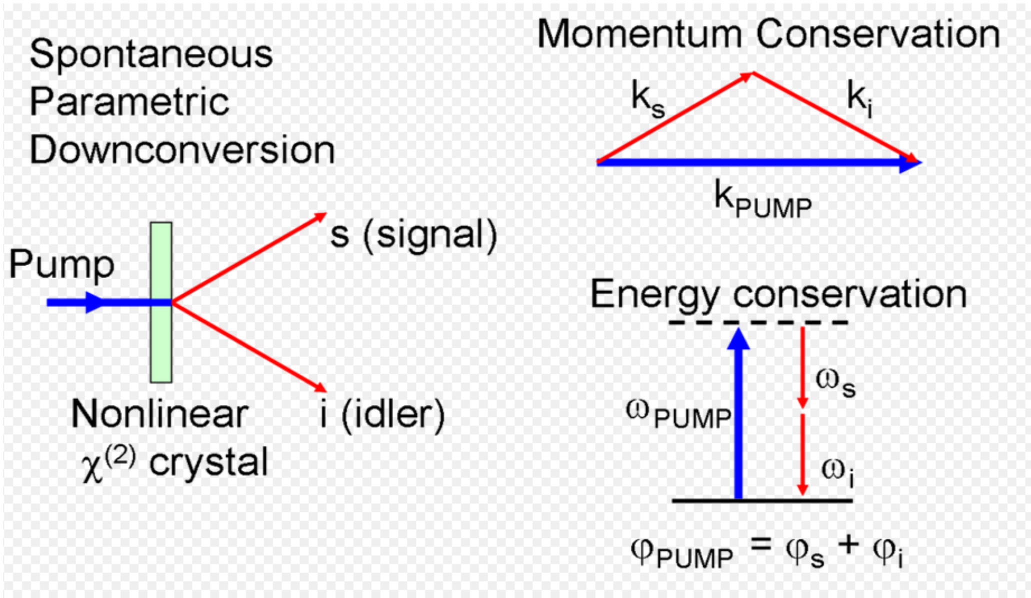

Fig. 2.5. Spontaneous parametric down-conversion [87]

2.1.4 Quantum Repeater Key Rate Analysis

Key rate or secret key rate (R) represent a figure of merit in quantum repeater operation, it is effectively the product of keys that can be extracted from a state which know as secret key fraction (r) and the yield of generating the state (Y). secret key fraction measures the state quality, and it's a function of quantum bit error rate QBER which is a measure of the probability that Alice and Bob using the same basis. The general equation measure the secrete key rate of quantum repeater is illustrated in (Eq. 2.5) [17, 20].

$$R_{\infty} = \frac{Y}{2}\left(1 - h[e_x] - fh[e_z]\right) \qquad \text{………..(2.5)}$$

where:

- Y : yield (bits per channel use).

- The factor of 1/2 corresponding to the fact that the protocol uses two polarization modes.
- h (e) : binary entropy function.
- $(1-h[e_x]-fh[e_z])$: classical error correction and privacy amplification protocols.
- e_x & e_z: QBER in the X and Z bases respectively.
- **f** : realistic inefficiency in error correction. For perfect error correction schemes $f=1$ and for non-perfect schemes $f>1$.

The yield (Y) represents the probability that the measurements done by Alice and Bob and the BSM were successful. It is inversely proportional relative to the number of channel uses and as shown in the following equation.

$$Y=\frac{p_{BSM}^{n}}{\sum_{k=0}^{k=\infty}\left(1-\left(1-(1-p_a)^k\right)\left(1-(1-p_b)^k\right)\Pi_{i=1}^{n-1}\left(1-(1-p_i)^k\right)\right)} \quad \text{……….(2.6)}$$

Where,

p_a & p_b: Alice & Bob success probability.

p_i: inner links success probability.

$$p_{a,b}=1-\left(1-\eta_{a,b}\right)\left(1-p_{dark}\right)^2 \quad \text{…………(2.7)}$$

$$\eta_{a,b}=\eta_{tot}e^{-L_{a,b}/L_{att}}$$

Quantum bit error rate QBER measure the error produced by the components of the system between Alice and Bob and can be summarized by the following equations:

$$e_z = \frac{1}{2} - \frac{(1-2e_M)^{2n}\lambda_{BSM}^{n}\alpha^2\mu_z^{n-1}}{2} \quad \text{.........(2.8)}$$

and

$$e_x = \frac{1}{2} - \frac{(1-2e_M)^{2n}\lambda_{BSM}^{n}\alpha^2\mu_x^{n-1}f_{dp}[n]}{2} \quad \text{.........(2.9)}$$

where,

e_x: QBER in X basis

e_z: QBER in Z basis

$f_{dp}[n]$: dephasing in QM

Dephasing parameter QM dephasing errors and expressed as:

$$f_{dp}[n] = E\left[e^{-\sum_{i=1}^{i=2n} t_i / T_2} \right] \quad \text{..........(2.10)}$$

Finally, the equation for secrete key rate is illustrated in the following equation [44].

$$R = \frac{Y}{2}\left(1 - fh[e_z] - h\cdot\left[\frac{1}{2} - \frac{(1-2e_M)^{2n}\lambda_{BSM}^{n}\alpha^2\mu_x^{n-1}}{2}\right.\right.$$
$$.e^{-\frac{2L_a+L_{inn}}{T_{21}c}}.e^{-\frac{(n-1)L_{inn}+2L_b}{T_{22}c}}.e^{-\frac{(2n-2)L_{inn}}{T_{23}c}}.\left[\frac{P_{OBSM}}{e^{\tau_p/T_{21}}+P_{OBSM}-1}\right].$$
$$\left.\left.\left[\frac{P_{OBSM}}{e^{\tau_p/T_{23}}+P_{OBSM}-1}\right]^{(n-2)}.\left[\frac{P_b}{e^{\tau_b/T_{23}}+P_b-1}\right]\right]\right) \quad \text{......(2.11)}$$

2.2 Power Consumption Model

The power consumption evaluation is necessary to model the energy efficiency of any network. However, why energy efficiency, this metric is recently used to examine the performance of the modern network at is holds the power consumption indicator. The power consumption of each proposed network has been calculated for a specific distance. As the distance is known, the required equipment that is required to fulfill this distance will be known too. Then, the power consumption of these devices is evaluated.

In this thesis, long distance has been assumed to show the effectiveness of all networks, that is 200km. This distance represents the distance of which the information to be traveled from Alice to Bob. In the full quantum network, the number of repeaters, quantum memories, photon detectors and central/control units has been examined. For the same distance, in the hybrid and classical case.

In the hybrid cases (optical and wireless), part of this channel is used by the classical base station, thus the participating devices will be a combination of quantum and classical networks. At the same time, deducting the quantity of the quantum devices in the classical distance, i.e. the one covered by classical channel.

Moreover, all classical network will not contain any quantum devices. Noticing that, the consumption of classical communications isn't really meant that the fully amount of calculated power will be considered in this work, because this work assumed the classical base station has been rented or cooperatively used together with the already existed traditional network operator. The same logic holds true with respect to the hybrid paradigm. Hence, borrowing the classical base station from the traditional network will not add a large amount of power consumption to the network in the hybrid design. Instead, it can offer an essential solution when the all quantum network faces a high cost. When Alice is attempting to communicate with the client Bob. The power consumption of such attempt will be computed. In which, the memory, detectors and lasers consumptions have been assumed to be about 2W. Another addition to this consumption is the control server unit that is unavoidable for controlling the entangled photons and synchronization.

This control server consumes at least 29 W, which includes the consumption of the overhead [88]. However, we assumed the consumption of the laser is P_{laser}, the memory is P_{memory} the detector is P_{det}, and the central unit is $P_{central}$. In addition, it has been mentioned in [89] that the entanglement photons can be exchanged without using the repeaters for maximum distance of 50km. Beyond this distance, it is not ensured the photons states will not be faded or attenuated. Subsequently, the consumption of the repeater is denoted as $P_{repeater}$, and can be given as

$$P_{repeater} = P_{central} + P_{det} + \mathrm{P}_{\mathrm{laser}} + P_{me} \quad \ldots\ldots\ldots\ldots(2.12)$$

For any distance, the required power consumption shall include the number of required devices in that particular distance and included several number of repeaters, as follows:

$$P_{repeater} = P_{central} + D * P_{det} + S * P_{laser} + M * P_{memory} \quad \ldots\ldots(2.13)$$

Where D is detector number, S represents the number of the sources, M is the quantity of the quantum memories.

In the hybrid case, the coverage of the classical base station range is about 25 km radius (50 km full coverage), after that distance, a classical amplifier is applied. let's assume that the classical distance that is required in the hybrid case is100 km, that is half the total distance (200 km). Subsequently, 4 base stations are required, each with 25 km coverage, as shown in Figure 2.6. Presently, we attempt to compute the consumption of this distance and mutually adding this to the next 100 km, which is covered by the quantum repeater.

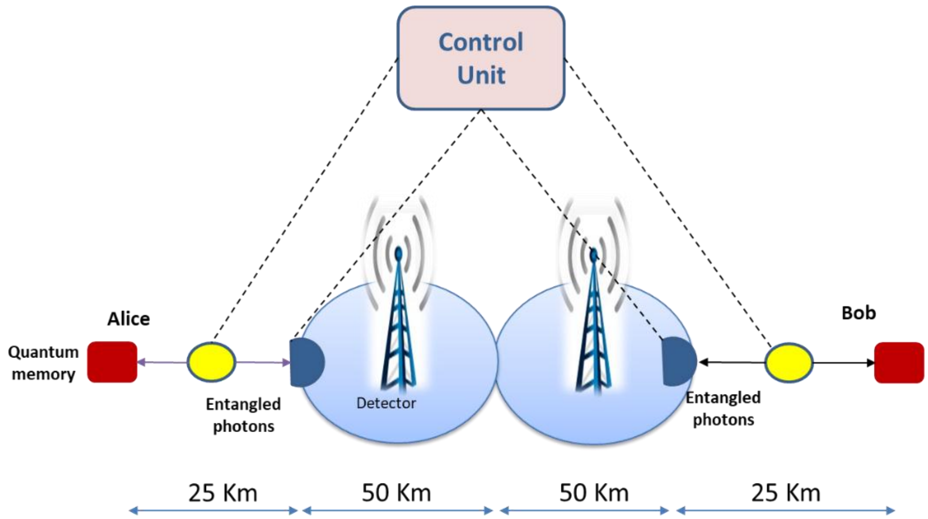

Fig. 2.6: The classical- quantum network paradigm to show the distances of eachproposed architecture.

The power consumption of the classical base station has been assigned as P_{BS}. This station included the following subsequent components: (1) base band server, which is a DSP unit responsible about the necessary features associated with signal processing, together with encoding, ciphering, deciphering, and sampling processes. Furthermore, this component is responsible of converting the transmitted or received signals to/from digital or analogue forms.

This base band unit is attached to (2) Radio frequency (RF) unit, which is responsible for signals' transmitting/receiving, and achieves modulation and demodulation processes. (3) Power amplifiers (PA) are needed to amplify the transmitted or received base band signals before sending them to the antennas. (4) There are still additional power consumptions which might be associated with cooling the base station, converting AC-DC, and then converting DC-DC power. These consumptions are usually assumed to be directly proportional to other energy consumers within the base station. Hence, the overall power consumption of the classical base station can be modeled as [90]:

$$P_{BS} = B * \frac{P_{PA}+P_{RF}+P_B}{Pcool * PDC * PAC} \qquad \ldots\ldots\ldots\ldots\ldots (2.14)$$

Where P_B denotes the power consumption of the base band unit server, B represents the quantity of the base stations. Subsequently, $P_{head} = P_{cool} * P_{DC} * P_{AC}$ can be given to combine the three power overhead consumers, these are cooling consumption P_{cool} DC to DC conversion power consumption P_{DC}, and AC to DC conversion power consumption P_{AC}. This power consumption is considered as losses, and it is a unitless.

In the Hybrid case, to examine the power consumption, the classical power consumption is jointly combined with the quantum power consumption, each with half the distance. Hence, the hybrid power consumption can be modeled as:

$$P_{hybrid} = P_{BS} + (D^h P_{det}) + \left(M^h P_{memory}\right) + P_{central} + (S^h P_{laser}) \qquad \ldots\ldots\ldots\ldots\ldots\ldots\ldots\ldots (2.15)$$

Where M^h, S^h, D^h, are the number of quantum memories, laser sources and photon detectors, respectively, within the hybrid network.

2.3 Hybrid Data rate modeling

Because the optical fiber has been used in most cases to transfer the quantum optical states, the available bandwidth is high because the laser light spectrum relies within the GHz frequencies. In contrast to the classical channel that uses the microwave signals, where the bandwidth is scarce, expensive, and lower than the optical channel. Hence, since the data rate is basically based up on the available bandwidth, it will be higher. Another solution the optical fiber links can offer is the immunity to interference that is originated by the other signals sources that can be found spatially at the same place of the original source.

First, the data rate of the system can be calculated using Shannon capacity. At a specific bandwidth, it can be given as [91]:

$$QRate_{optical} = BW\ log_2\ \left(1 + \frac{P_{laser}^{T}}{L}\right) \qquad \text{………………. (2.16)}$$

As L represents loss budget of the optical fiber channel. This loss is based on how far the channel is, i.e. the distance. In addition, it is based on the connectors number, number of splices, etc.

The link loss budget can be written as $P_{laser}^{R} = P_{laser}^{T} - L$, where P_{laser}^{R} denotes the power received, while P_{laser}^{T} represents the power transmitted of the laser source. Note that, this formula has been considered to calculate the data rate in all quantum case. However, the data rate of the quantum wireless can be calculated as [92]:

$$QRate_{wireless} = BW\ log_2 \left(1 + \frac{P_e h_{e,d} r_{e,d}}{BW\ N_o}\right) \qquad \text{……..……….. (2.17)}$$

Where the signal fading is represented by $h_{e,s}$ from entanglement source e to the detector d, P_e denotes the transmitted power of the entanglement source e when it is subjected to the noise N_o. The letter is called the additive white Gaussian noise and it is commonly used in the communication systems. Furthermore, $r_{e,d} = d_q^{-\propto}$ symbolizes the path loss of the channel that is affected by the quantum distance d_q, and α denotes the constant of the path loss. Subsequently, the classical wireless capacity has been formulated, as follows [92]:

$$WRate = BW\ log_2\left(1 + \frac{P_b h_b r_b}{BW\ N_o}\right) \quad \text{………………. (2.18)}$$

Where the signals fading is represented by h_b, P_b denotes the transmitted power of the base station b. Moreover, $r_b = d_b^{-\propto}$ symbolizes the path loss of the channel that is affected by the distance to the base station d_b. The differences between this channel and the quantum channel relies in the parameters of this formula. For example, the bandwidth in the wireless channel is less because it the microwave spectrum. In addition, the level of transmitted signal can be different, the interference from other signals and the inherent noise. All these factors can affect the result of the capacity.

2.4. Energy Efficiency modelling

In general, the energy efficiency can be evaluated as the data rate transmitted (bits/sec) or (bps) while consuming 1 Watt of power. Energy efficiency is a robust parameter in the communications metrics because it allows the network operators to examine the power consumption and the data rate at the same time. In general, the energy efficiency (EE) is given as [93]:

$$EE = \frac{Data\ rate}{Power\ consumption} \text{…………………….. (2.19)}$$

This is in consequence to the fact that the network sometimes can offer high data rates, but the network consumes a large amount of power at the same time. Hence, the energy efficiency can measure this network characteristic. As the formula stated, some parameters can affect the output of the energy efficiency. These parameters are the transmitted power, power consumption, noise, signal bandwidth and channel interference.

Now it is possible to model the energy efficiency of all quantum network ($EE_{quantum}$), as follows [94]:

$$EE_{quantum}^{optical} = EE_{quantum} = \frac{QRate_{optical}}{P_{repeater}} \quad \text{........ (2.20)}$$

This formula is applied to the optical quantum network too. Moreover, the quantum wireless energy efficiency is formulated as:

$$EE_{quantum}^{wireless} = \frac{QRate_{wireless}}{P_{repeater}} \quad \text{............... (2.21)}$$

In addition, the classical wireless energy efficiency ($EE_{Wireless}$) is calculated using same style [94]:

$$EE_{Wireless} = \frac{WRate}{P_{BS}} \quad \text{................................ (2.22)}$$

2.4.1 Hybrid Energy Efficiency

In hybrid network,the photons are transferred using two types of channels, quantum and classical. However, there are two types within the quantum case, which produces two types of hybrid networks:

A- Quantum optical- classical wireless

This type of network when the quantum part of the network uses optical fiber to transfer the photons, and the classical channel uses wireless too, its energy efficiency can be calculated using the following formula:

$$EE_{hybrid}^{optical} = \left|EE_{quantum}^{optical}\right|_{ZdN} + \left|EE_{wireless}\right|_{VdN} \quad \text{.......... (2.23)}$$

Where the total network distance is denoted by dN , Z is the quantum channel share of the distance, and V is the wireless channel share, both$V$ and Z are equal to 0.5 dN.

B- Quantum wireless- classical wireless

This type of network when both quantum and classical parts of the network uses wireless channel to transfer the photons, its energy efficiency can be calculated using the following formula:

$$EE_{hybrid}^{wireless} = \left|EE_{quantum}^{wireless}\right|_{ZdN} + |EE_{wireless}|_{VdN} \quad \text{……….(2.24)}$$

2.5 Methodology

As mentioned in previous sections in this study, quantum memory play a great role in the performance of quantum repeater, the most important parameters of the quantum memory which affected the quantum repeater performance are the decoherence time $\mathbf{T_2}$ and the coupling efficiency η_c , therefore, in this study the performance of the quantum repeater will examined by using three different quantum memories that are experimentally fabricated as shown in table 2.1.

Table 2.1 Quantum memory characteristics

	T_2 (s)	η_c	Reference
QM_1	16	0.78	[95, 96]
QM_2	0.1	0.73	[97, 98]
QM_3	0.018	0.9	[97]

A. in the case of single node quantum repeater (QR) the following steps is performed.

1. The key rate of the quantum repeater is calculated using the QMs mentioned in table (2.1) individually.

2. The decoherence time is fixed to (16s) while coupling efficiency be variable (0.78, 0.73, and 0.9).

3. Repeat step (2) to the other two decoherence times.

4. The coupling efficiency is fixed to (0.78) while decoherence time be variable (16s, 0.1s, and 0.018s).

5. Repeat step (4) to the other two coupling efficiency.

Steps (2-5) was performed to check which parameter affected the key rate of the quantum repeater more than the other one (i.e. T_2 or η_c).

B. For the multi node quantum repeater the following steps were performed..

1. The key rate of the quantum repeater is calculated using the QMs mentioned in table (2.1) individually.

2. The decoherence time is fixed to (16s) while coupling efficiency be variable (0.78, 0.73, and 0.9).

3. Repeat step (2) to the other two decoherence times.

4. The coupling efficiency is fixed to (0.78) while decoherence time be variable (16s, 0.1s, and 0.018s).

5. Repeat step (4) to the other two coupling efficiency.

Steps (2-5) was performed to check which parameter affected the key rate of the quantum repeater more than the other one (i.e. T_2 or η_c).

C. Finally, the performance of Hybrid system is examined through calculating the following parameters.

1. Power consumption with various detectors number and with different numbers of lasers.
2. Data rate with respect to both transmitted power and bandwidth.
3. Energy efficiency calculation.

Chapter Three

Results & Discussion

The results obtained from the steps mentioned in methodology will illustrated in this chapter, all these results obtained by using Python 3.6 language.

3.1. Single node quantum repeater

1. the secret key rate of the quantum repeater is measured using three different quantum memories (Table 2.1) individually, as shown in table (3.1) and figure (3.1).

Table (3.1) Key rate of single node quantum repeater using three different quantum memories.

Distance (km)	R_1 (QM_1)	R_2 (QM_2)	R_3 (QM_3)
0	0.4	0.4	0.4
100	0.4	0.38	0.3
200	0.4	0.35	0.15
300	0.4	0.22	0.03
400	0.4	0.07	0
500	0.39	0	0
600	0.35	0	0
700	0.17	0	0
800	0.06	0	0
900	0	0	0

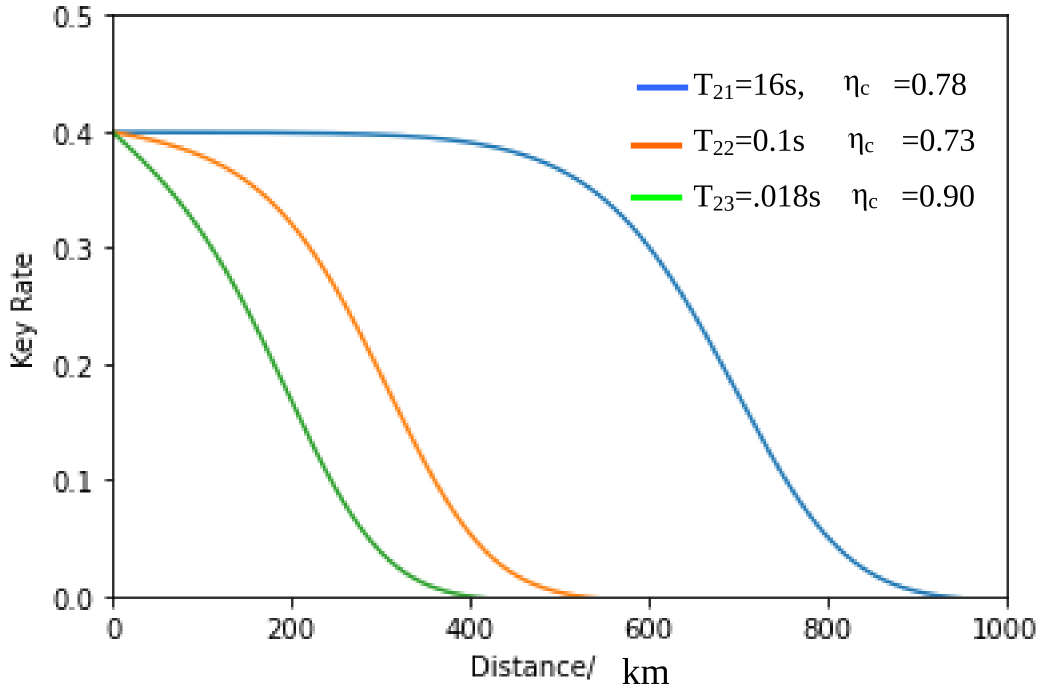

Fig. 3.1. Key rate of single node quantum repeater using three different quantum memories.

From (Fig. 3.1) it's clear that the amount of key rate is independent upon the characteristics of quantum memory since it is the same for all the three different types of quantum repeater, while the distance that the quantum state reach before decay to zero is depend upon the characteristics of quantum memory especially the decoherence time T_2 as it reach about 900km when using quantum memory with 16s decoherence time while reaching about 500km when using quantum memory with decoherence time 0.1 s and finally it reaches about 400km by using a quantum memory with decoherence time 0.18s. all this results agrees with aim of using quantum repeater which is used to extend the distance and overcome the problem of exponential decay of quantum state in the case of direct transmission.

2. In this step the quantum repeater performance is examined when the decoherence time is assumed to be the same for the quantum memories

while the coupling efficiency is varying using values illustrated in table (2.1). the results obtained illustrated in table (3.2) and Fig (3.2).

Table (3.2) Key rate of single node quantum repeater using three different quantum memories.

Distance (km)	R (T_2=16s)	R (T_2=0.1 s)	R (T_2=0.018s)
0	0.4	0.4	0.4
100	0.4	0.38	0.3
200	0.4	0.35	0.13
300	0.4	0.2	0.04
400	0.4	0.06	0
500	0.39	0	0
600	0.3	0	0
700	0.2	0	0
800	0.06	0	0
900	0	0	0

(a)

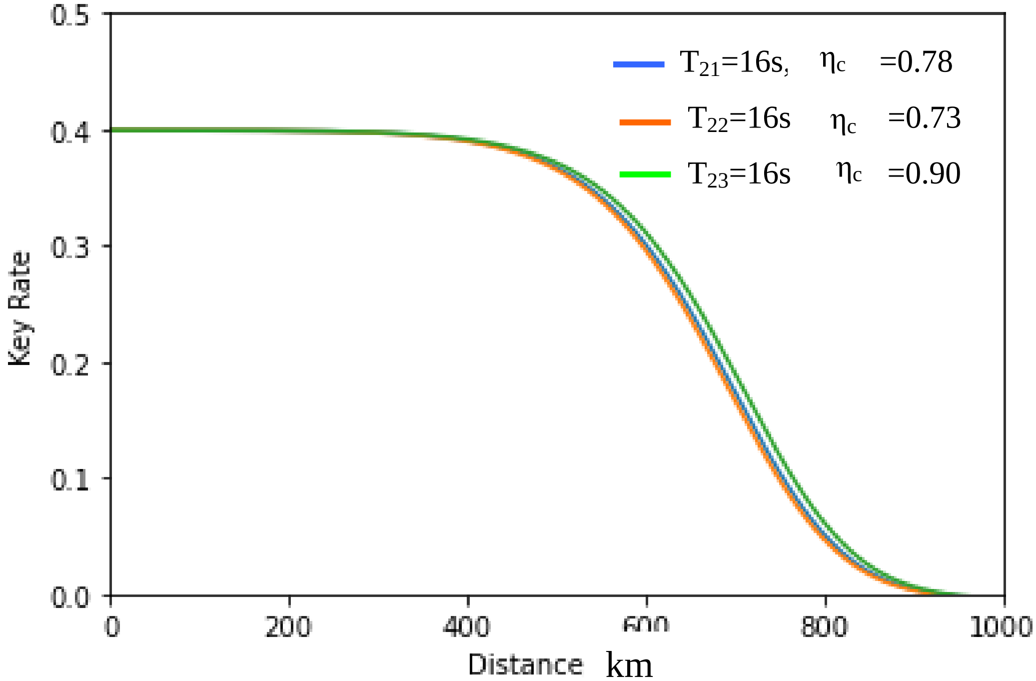
T21=16s, ηc =0.78
T22=16s ηc =0.73
T23=16s ηc =0.90
Key Rate
Distance km
0.5
0.4
0.3
0.2
0.1
0.0
0
200
400
600
800
1000

(b)

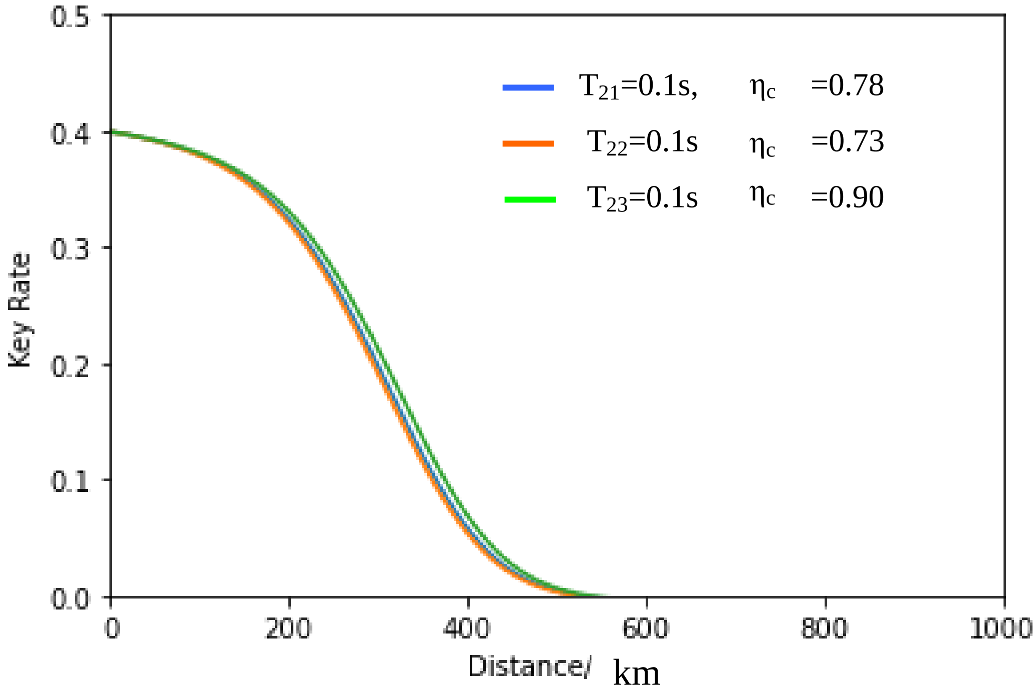
T21=0.1s, ηc =0.78
T22=0.1s ηc =0.73
T23=0.1s ηc =0.90
Key Rate
Distance/ km
0.5
0.4
0.3
0.2
0.1
0.0
0
200
400
600
800
1000

(c)

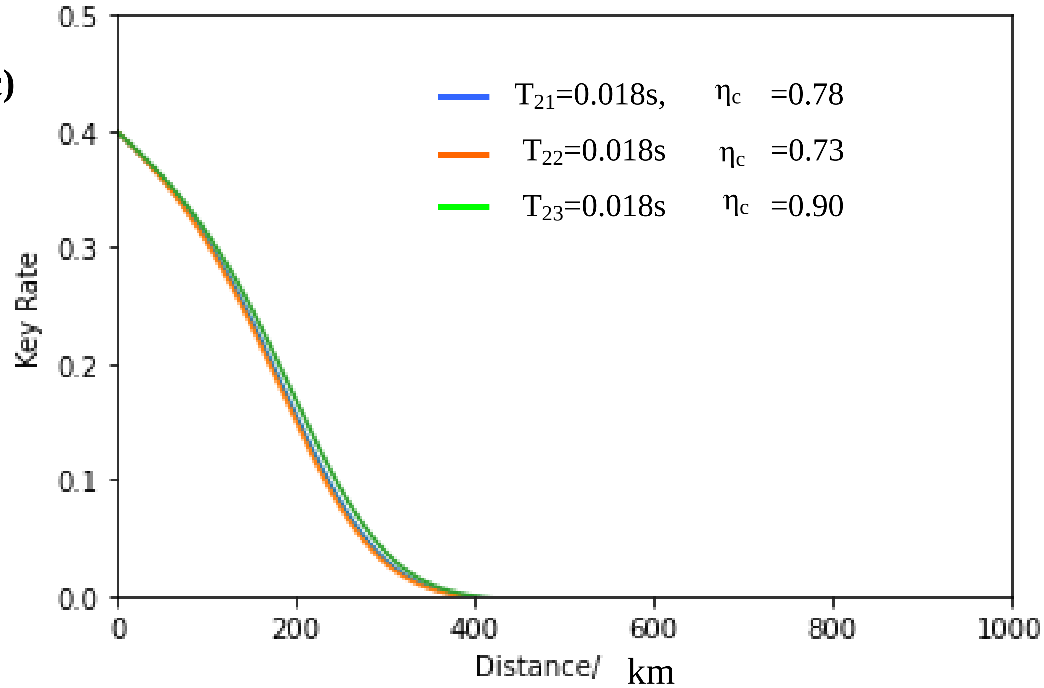

Fig. 3.2. Key rate of quantum repeater using three different quantum memories. (a) T_2 = 16 s , (b) T_2 = 0.1 s , (c) T_2 = 0.018s

From Fig. (3.2) it is clear that if a long decoherence time quantum memory is used then the distance that the quantum state can be transmitted to is increased and this agrees with results obtained in step (1) in this procedure.

3. In this step the quantum repeater performance is examined when the coupling efficiency of the quantum memories used in this study is assumed to be the same, while the decoherence time is varying using values in table (2.1). The results obtained illustrated in table (3.3) and Fig. (3.3).

Table (3.3) Key rate of single node quantum repeater using three different quantum memories.

Distance (km)	R_1 (QM_1)	R_2 (QM_2)	R_3 (QM_3)	R_1 (QM_1)	R_2 (QM_2)	R_3 (QM_3)	R_1 (QM_1)	R_2 (QM_2)	R_3 (QM_3)
	η_c = 0.78			η_c = 0.73			η_c = 0.9		
0	0.4	0.4	0.4	0.4	0.4	0.4	0.4	0.4	0.4
100	0.4	0.39	0.33	0.4	0.39	0.35	0.4	0.38	0.35
200	0.4	0.34	0.17	0.4	0.33	0.15	0.4	0.34	0.16
300	0.4	0.21	0.02	0.4	0.2	0.03	0.4	0.22	0.05
400	0.4	0.05	0	0.4	0.05	0	0.4	0.08	0
500	0.39	0	0	0.39	0	0	0.38	0	0
600	0.35	0	0	0.32	0	0	0.35	0	0
700	0.18	0	0	0.15	0	0	0.2	0	0
800	0.06	0	0	0.04	0	0	0.06	0	0
900	0	0	0	0	0	0	0	0	0

(a)

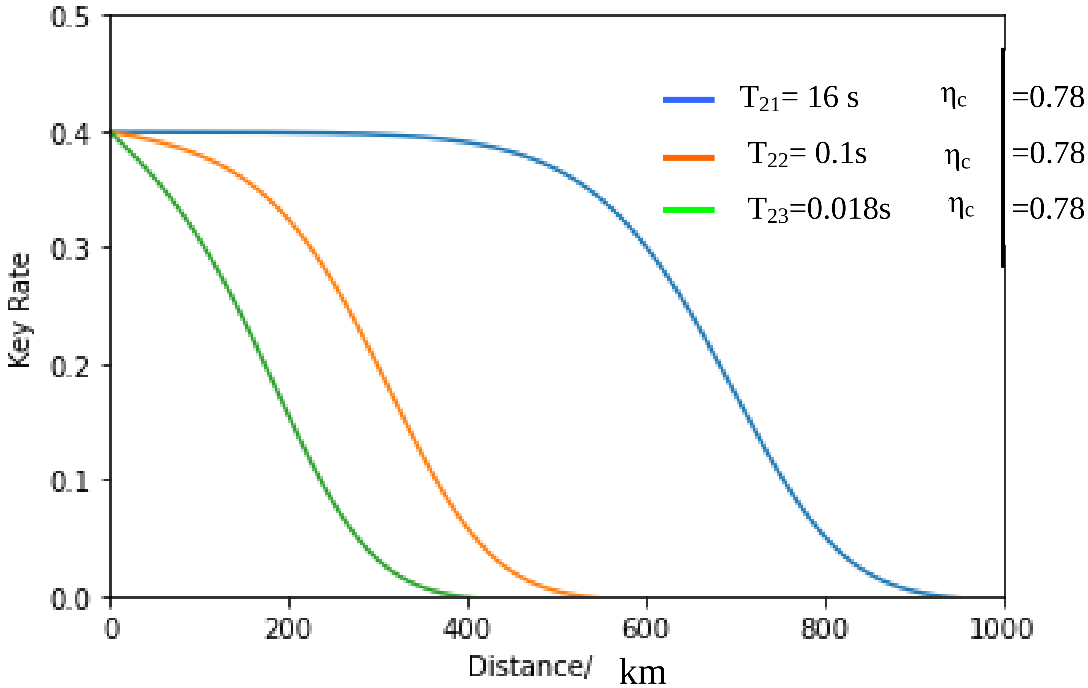
0.5
0.4
0.3
0.2
0.1
0.0
Key Rate
0
200
400
600
800
1000
Distance/ km
T21= 16 s ηc =0.78
T22= 0.1s ηc =0.78
T23=0.018s ηc =0.78

(b)

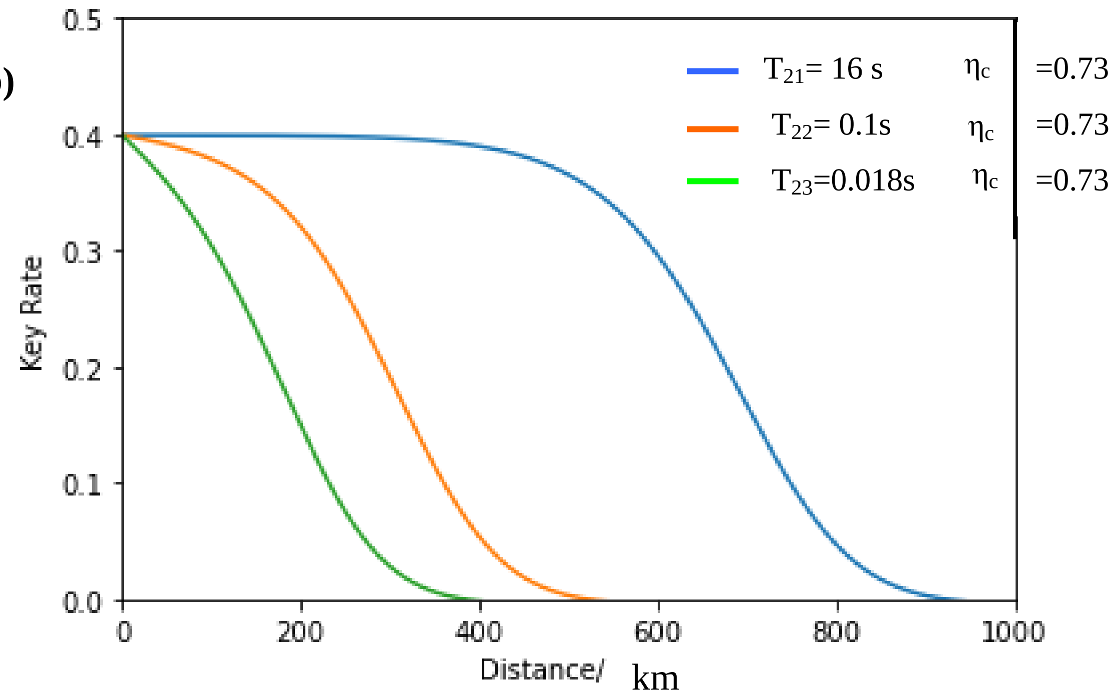
0.5
0.4
0.3
0.2
0.1
0.0
Key Rate
0
200
400
600
800
1000
Distance/ km
T21= 16 s ηc =0.73
T22= 0.1s ηc =0.73
T23=0.018s ηc =0.73

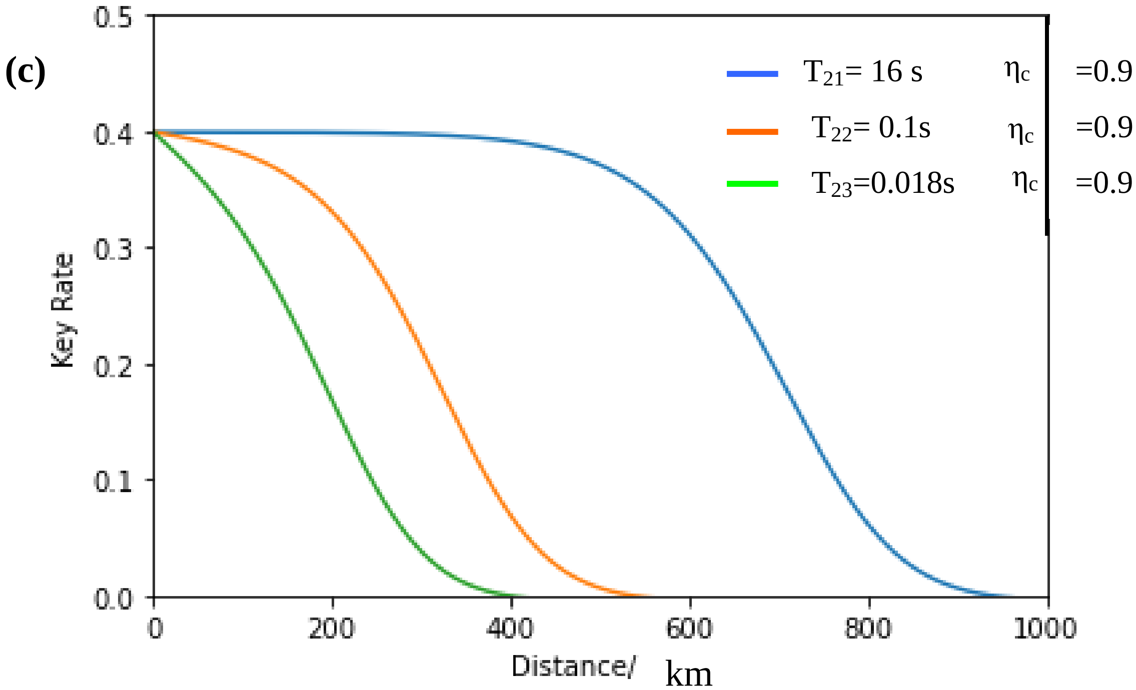

Fig. 3.3. Key rate of quantum repeater using three different quantum memories. (a) η_c = 0.78 , (b) η_c = 0.73 , (c) η_c = 0.9

The results shown in Fig. (3.3) shows that both the ker rate and the distance that the quantum state can reach before dcay is the same even if the coupling efficieny of the quantum memory is changed and using quantum memory with longest decoherence time give the longest distance.

3.2. Multi node quantum repeater.

1. In this step, the procedure used in single node quantum repeater is repeated but for multi node quantum repeater. Firstly, number of nodes (n) will be (n=3), the results obtained id shown table (3.4) and Fig. (3.4).

Table (3.4) Key rate of multi node quantum repeater using three different quantum memories. (n=3)

Distance (km)	R_1 (QM_1)	R_2 (QM_2)	R_3 (QM_3)
0	3.4	0.32	0.39
100	0.3	0.25	0.15
200	0.3	0.15	0.025
300	0.3	0.025	0
400	0.29	0	0
500	0.25	0	0
600	0.1	0	0
700	0.03	0	0
800	0	0	0
900	0	0	0

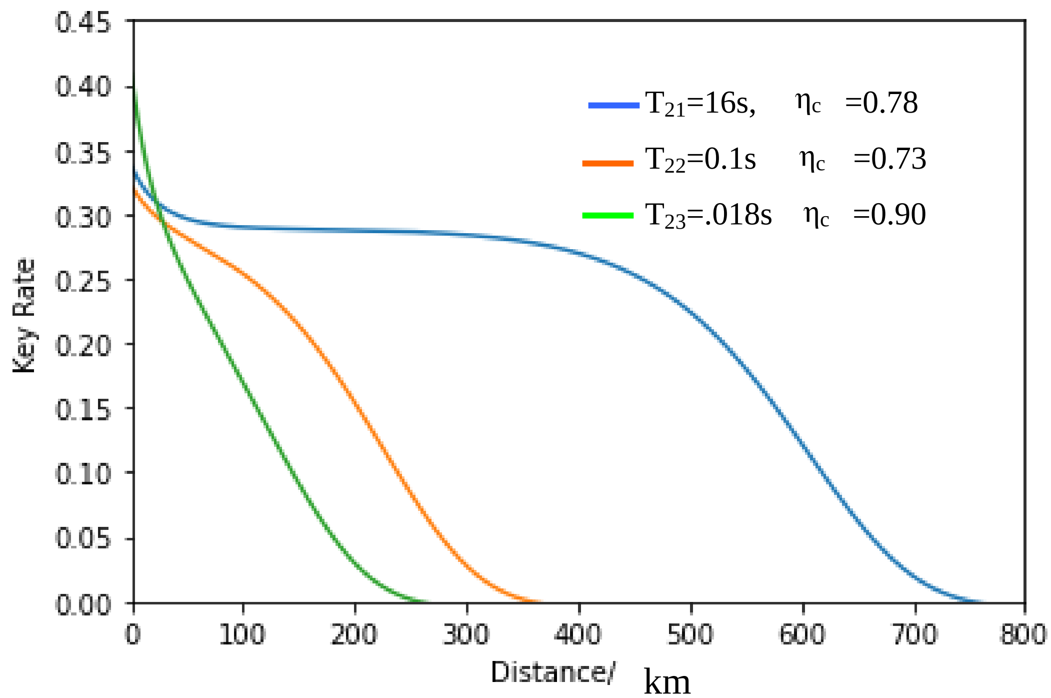

Fig. 3.4. Key rate of multi node (n=3) quantum repeater using three different quantum memories.

From (Fig. 3.4) it's clear that the distance that the quantum state reach before decay to zero is depend upon the characteristics of quantum memory especially the decoherence time T_2 as it reach about 800km when using quantum memory with 16s decoherence time while reaching about 400km when using quantum memory with decoherence time 0.1 s and finally it reaches about 300km by using a quantum memory with decoherence time 0.18s, and if we compare these distances with that obtained in the single node quantum repeater (Fig. 3.1) it is easily observed that its less and this due to the imperfections introduced by the components used in the quantum repeater since multi node quantum repeater consists of more components than single node repeater.

2. In this step the multi node (n=3) quantum repeater performance is examined when the decoherence time is assumed to be the same for the

quantum memories while the coupling efficiency is varying using values illustrated in table (2.1). the results obtained illustrated in table (3.5) and Fig (3.5).

Table (3.5) Key rate of multi node quantum repeater using three different quantum memories. (n = 3)

Distance (km)	R_1 (QM_1)	R_2 (QM_2)	R_3 (QM_3)	R_1 (QM_1)	R_2 (QM_2)	R_3 (QM_3)	R_1 (QM_1)	R_2 (QM_2)	R_3 (QM_3)
	T_1 = 16 s			T_2 = 0.1 s			T_3 = 0.018s		
0	0.34	0.33	0.4	0.34	0.33	0.39	0.33	0.33	0.39
100	0.3	0.3	0.3	0.25	0.25	0.26	0.14	0.14	0.17
200	0.3	0.3	0.3	0.15	0.15	0.17	0.015	0.015	0.03
300	0.3	0.3	0.3	0.03	0.03	0.05	0	0	0
400	0.3	0.3	0.3	0	0	0	0	0	0
500	0.23	0.230.23	0.25	0	0	0	0	0	0
600	0.1	0.1	0.15	0	0	0	0	0	0
700	0.02	0.02	0.05	0	0	0	0	0	0
800	0	0	0	0	0	0	0	0	0
900	0	0	0	0	0	0	0	0	0

(a)

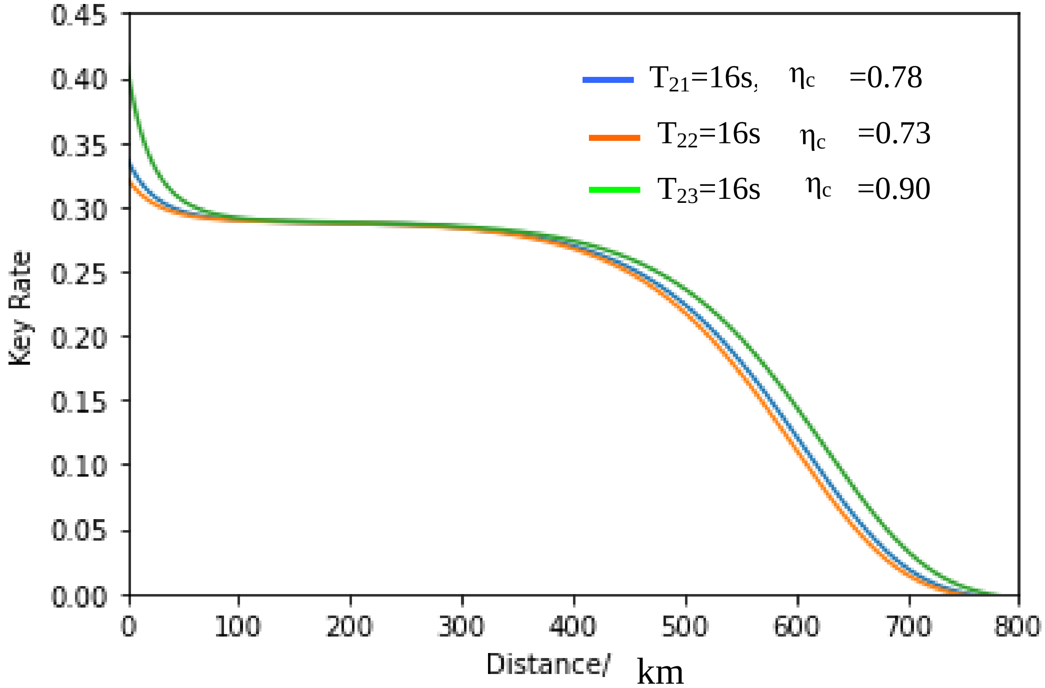
0.45
0.40
0.35
0.30
0.25
0.20
0.15
0.10
0.05
0.00
Key Rate
0
100
200
300
400
500
600
700
800
Distance/ km
T_{21}=16s, η_c =0.78
T_{22}=16s η_c =0.73
T_{23}=16s η_c =0.90

(b)

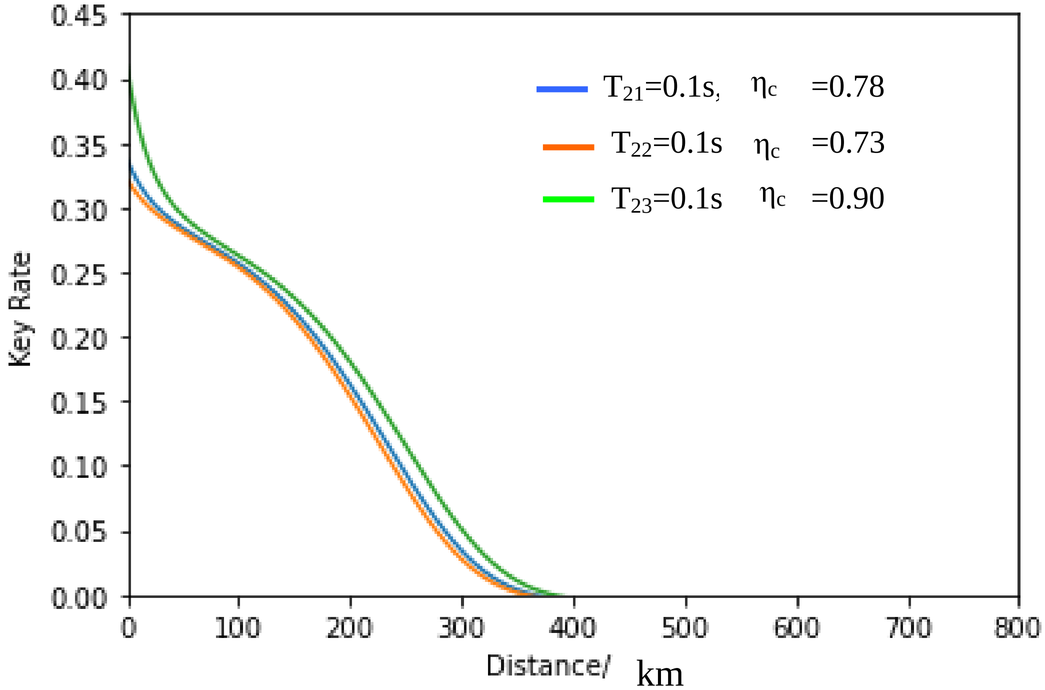
0.45
0.40
0.35
0.30
0.25
0.20
0.15
0.10
0.05
0.00
Key Rate
0
100
200
300
400
500
600
700
800
Distance/ km
T_{21}=0.1s, η_c =0.78
T_{22}=0.1s η_c =0.73
T_{23}=0.1s η_c =0.90

(c)

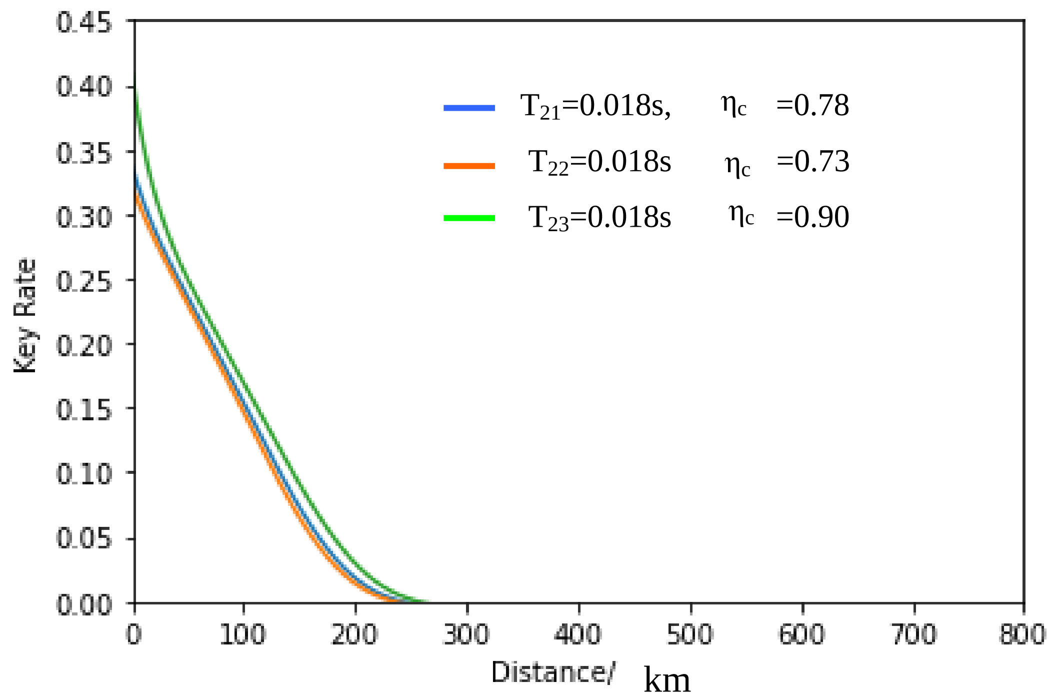

Fig. 3.5. Key rate of multi node (n=3) quantum repeater using three different quantum memories. (a) T_2 = 16 s , (b) T_2 = 0.1 s , (c) T_2 = 0.018s

From Fig. (3.5) it is clear that if a long decoherence time quantum memory is used then the distance that the quantum state can be transmitted to is increased, while using quantum memories with less decoherence time will decrease the distance that quantum state can reach.

3. In this step the multi node (n=3) quantum repeater performance is examined when the coupling efficiency of the quantum memories used in this study is assumed to be the same, while the decoherence time is varying using values in table (2.1). The results obtained illustrated in table (3.6) and Fig. (3.6), which approved that both the key rate and the distance that the quantum state can reach before dcay is the same even if the coupling efficieny of the quantum memory is changed and using quantum memory with longest decoherence time give the longest distance.

Table (3.6) Key rate of multi node quantum repeater using three different quantum memories. (n = 3)

Distance (km)	R_1 (QM_1)	R_2 (QM_2)	R_3 (QM_3)	R_1 (QM_1)	R_2 (QM_2)	R_3 (QM_3)	R_1 (QM_1)	R_2 (QM_2)	R_3 (QM_3)
	η_c = 0.78			η_c = 0.73			η_c = 0.9		
0	0.37	0.37	0.37	0.32	0.32	0.32	0.39	0.39	0.39
100	0.3	0.27	0.13	0.3	0.26	0.12	0.3	0.25	0.15
200	0.3	0.16	0.02	0.3	0.15	0.01	0.3	0.17	0.02
300	0.3	0.03	0	0.3	0.03	0	0.3	0.04	0
400	0.39	0	0	0.29	0	0	0.29	0	0
500	0.25	0	0	0.23	0	0	0.24	0	0
600	0.14	0	0	0.13	0	0	0.14	0	0
700	0.03	0	0	0.015	0	0	0.04	0	0
800	0	0	0	0	0	0	0	0	0
900	0	0	0	0	0	0	0	0	0

(a)

(b)

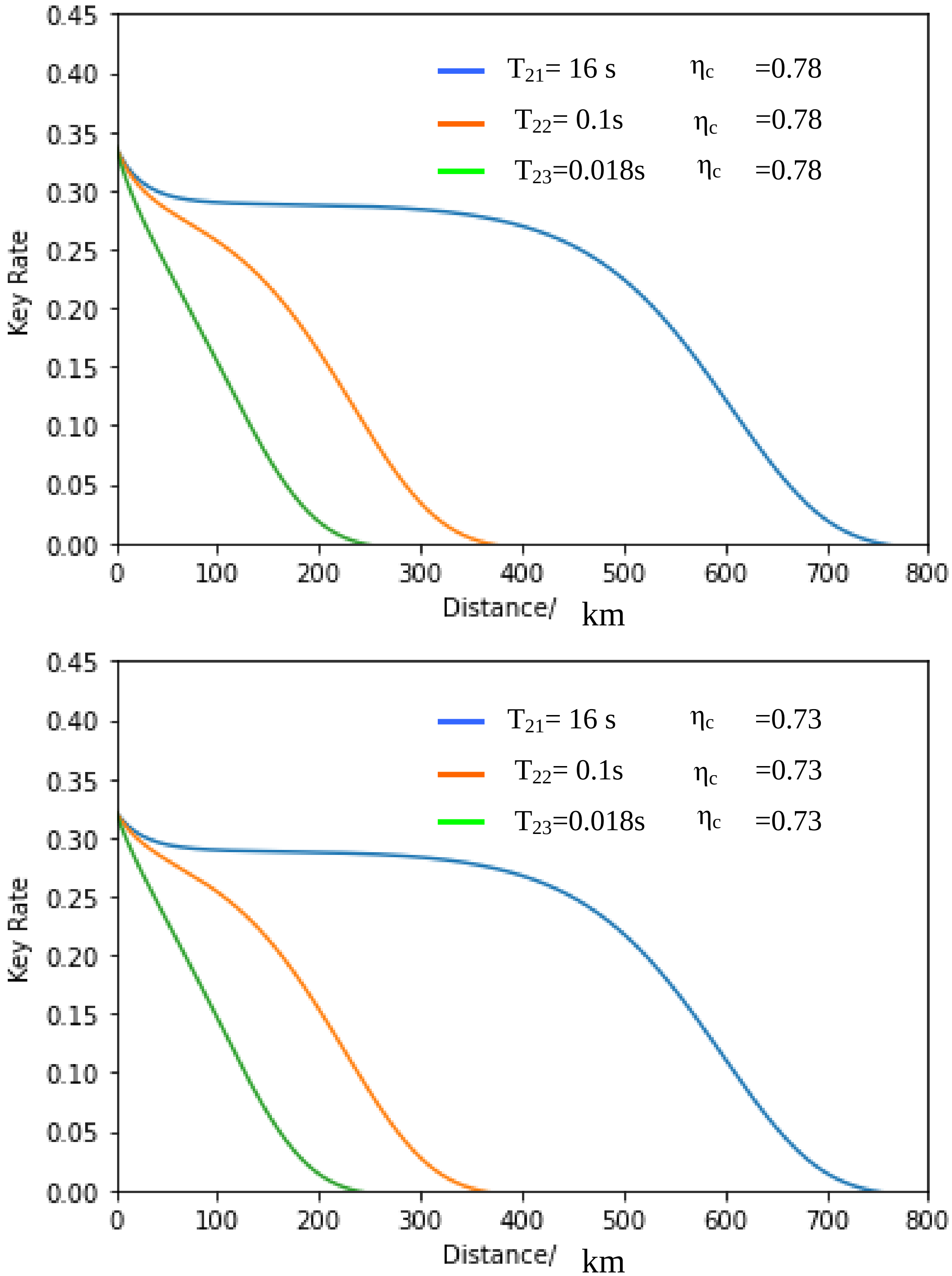
T_{21}= 16 s η_c =0.78
T_{22}= 0.1s η_c =0.78
T_{23}=0.018s η_c =0.78
Key Rate
Distance/ km
T_{21}= 16 s η_c =0.73
T_{22}= 0.1s η_c =0.73
T_{23}=0.018s η_c =0.73
Key Rate
Distance/ km

(c)

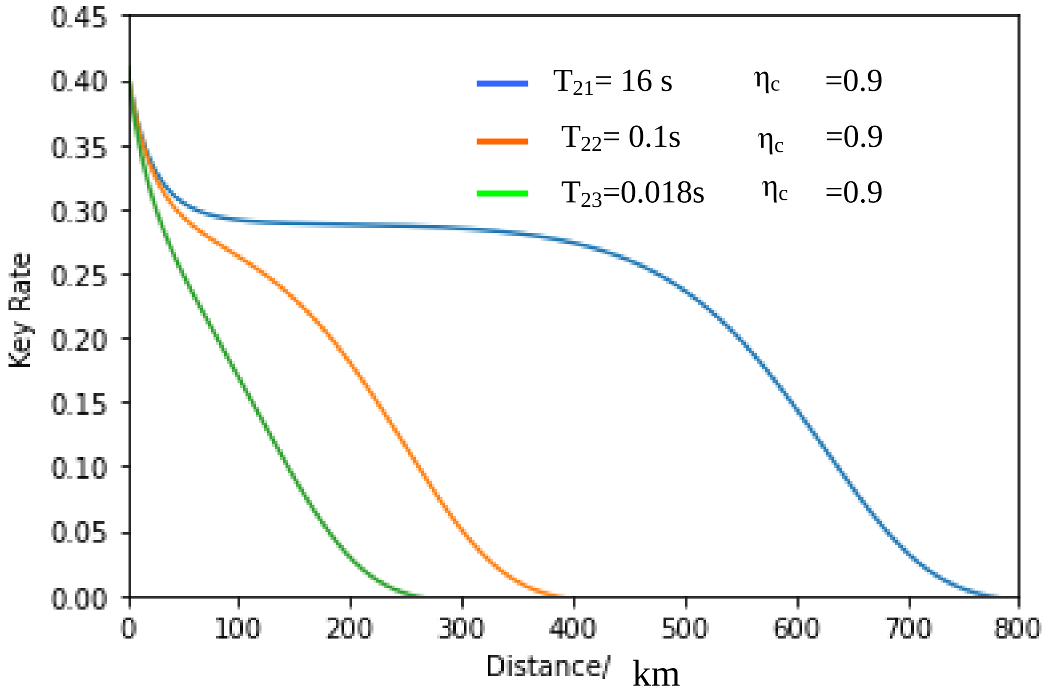

Fig. 3.6. Key rate of multi node (n=3) quantum repeater using three different quantum memories. (a) η_c = 0.78 , (b) η_c = 0.73 , (c) η_c = 0.9

3.3 Hybrid system data rate results

3.3.1 Power consumption calculation.

Figure 3.7 shows the power consumption of the all quantum and hybrid network with different amount of detectors. It should be noted that 8 detectors are used in all quantum system and only 4 are used in the hybrid system. The laser's number is also the same. The all-classical case was excluded from this comparison as its power consumption will be more that all the mentioned cases and doesn’t contain any detectors in its design.

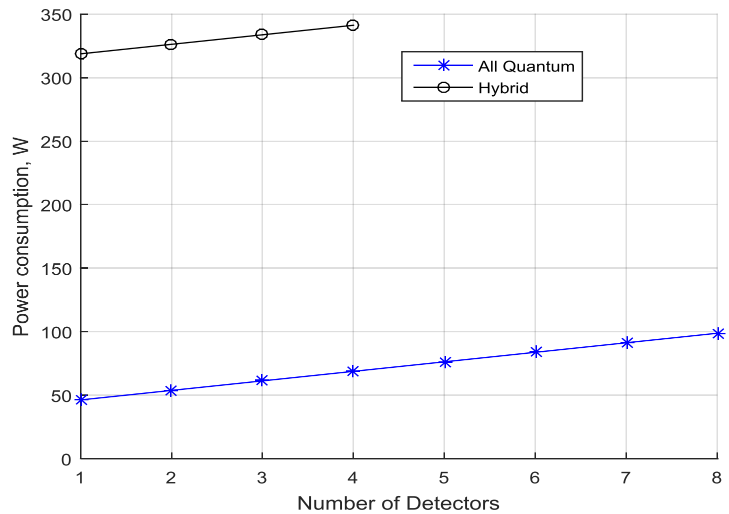

Fig 3.7: Power consumption comparison of quantum and hybrid case with variousdetectors number.

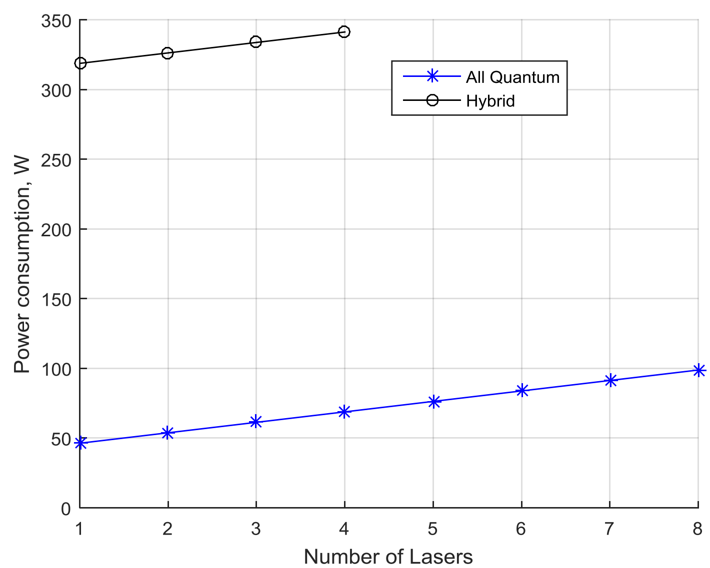

Figure 3.8: Power consumption comparison of all quantum and hybrid network with different number of lasers.

Figure 3.8 shows the power consumption comparison of all quantum and hybrid network with different number of lasers, this result shows the same behavior as the previous result.

The power consumption of the hybrid case is higher than the fully quantum case. However, we have assumed the classical base station is fully owned. Hence, all the base station power consumption has been added to the hybrid case. This results in upgrading the power consumption of the hybrid case and advocating against its power performance.

3.3.2 Data rate calculation.

To calculate the data rate, it was assumed there are 100 users, and their sum data rate will be calculated. As the frequency of the entangled photon owns higher bandwidth, this means more bit rate will be transmitted as per Shannon theory.

Figure 3.9 shows a comparison of the channel capacity for the hybrid, classical and all quantum network with respect to the base station transmitted power. Note that the hybrid case includes both wireless quantum and optical quantum networks.

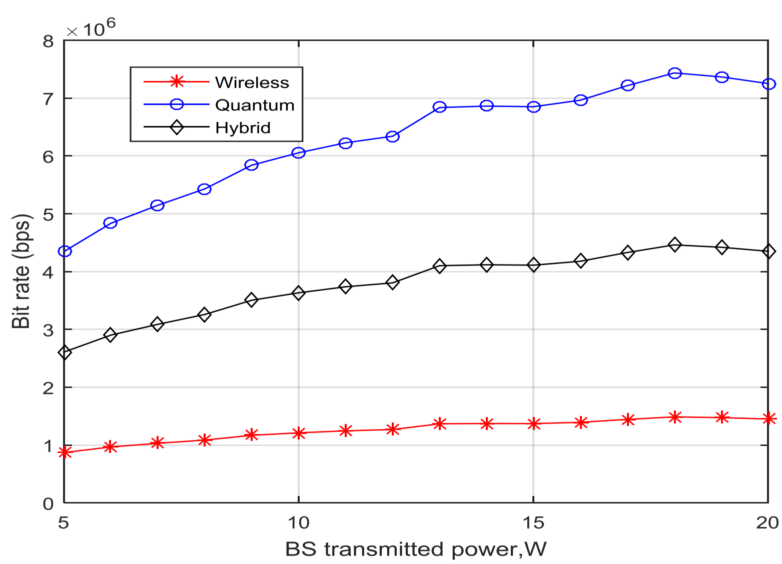

Fig 3.9: Bit rate comparison of the all quantum, classical and hybrid systems with respect to the transmitted power.

The all quantum case has scored higher bit rate as their channel is purely optical or wireless with high bandwidth, which increases the data rate. In the hybrid case, part of the channel has been a classical wireless, which has less bandwidth than the all quantum case. Finally, the all classical case has lower frequency and bandwidth that forces the data rate to become the least.

Figure 3.10 shows the bit rate comparison of the wireless, hybrid and quantum systems with regards to the available bandwidth, clearly when the bandwidth increases, the data rate increases too. This is however, is explained by Shannon capacity.

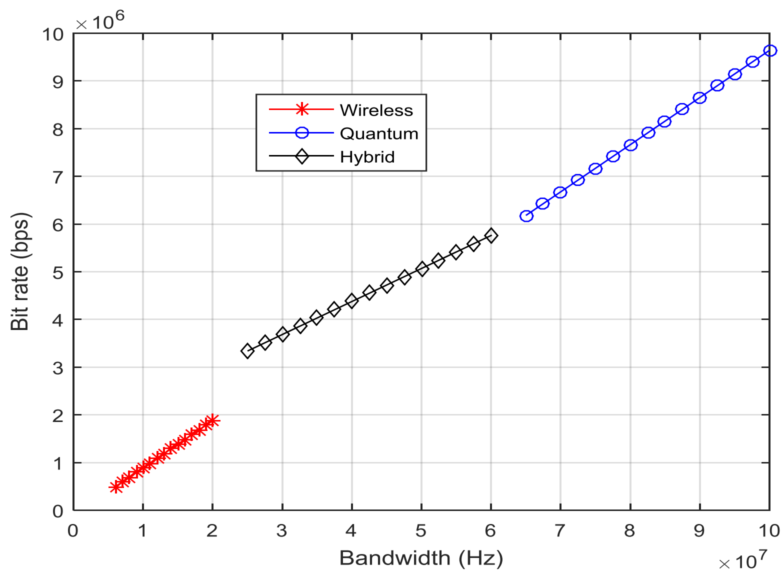

Fig. 3.10: Bit rate comparison of the quantum, classical and hybrid systems with respect to the bandwidth.

3.3.3 Power efficiency calculation.

To calculate the power efficiency, it was assumed 20 MHz the bandwidth, available every 0.5 ms, also named time slot in classical communications, and usually converted to 100 resource blocks to be sent to the users. Every resource block is equal to 180 KHz. These resource blocks are then utilized to be sent to the network subscribers and provide the necessary data. In a quantum system, the ultraviolet high frequency offers a bandwidth of about $1.9 \pm 0.00005 \times 10^5$ GHz, which is then translated to 100 MHz at a sufficient repetition rate. With less power consumption and large data rate of a quantum system, its energy efficiency becomes higher. Figure 3.11 shows the hybrid, classical, and quantum energy efficiencies. It shows the impact of the higher energy consumption in the hybrid, quantum, and traditional systems on energy efficiency.

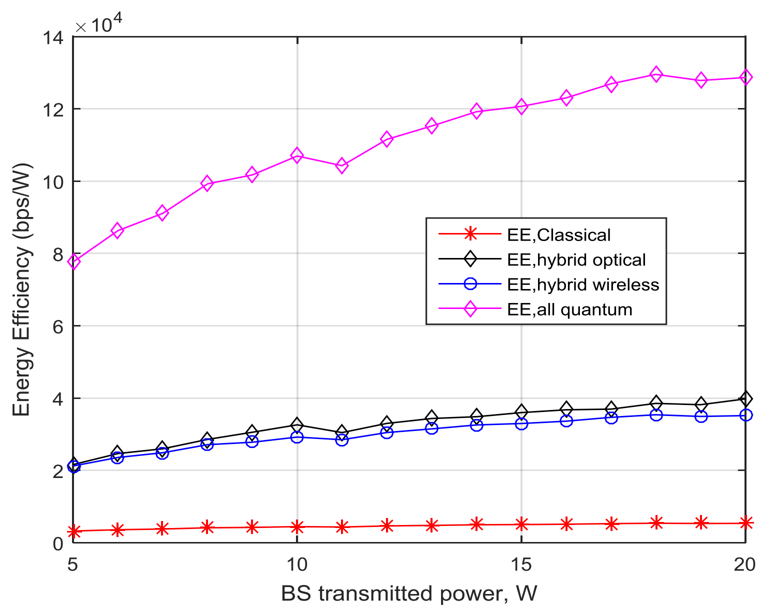

Fig. 3.11: Energy efficiency comparison of classical, hybrid, and quantum networks.

3.4 Conclusions

1. The performances of quantum repeater use quantum memories with long decoherence time is better that that use short decoherence time quantum memories.
2. Using quantum memories with high coupling efficiency improving the performance of quantum repeater.
3. Increasing number of nodes of the quantum repeater will decrease the distance that information can reach.
4. The power consumption of the hybrid case is higher than the fully quantum case.
5. The all quantum channel performance is better than that of hybrid channel.
6. The quantum system energy efficiency is higher than that of the hybrid system.

3.5 Future Work

1. Implementing this study practically to discover the effect of any other parameters on quantum repeater performance.
2. Designing quantum memories that have both decoherence time and coupling efficiency with large values.
3. Study the performance of quantum repeater using decoy state instead of EPR state.
4. Study the quantum repeater performance using free space channels.

References

References

[1] Svore K. M. and M. Troyer. The Quantum Future of Computation, Computer 49, 9, 21-30 (2016).

[2] Imre S., F. Balazs . Quantum Computing and Communications. John Wiley & Sons Ltd, England (2005).

[3] Miranda M. Classical communication problems solved using quantum entanglement (2008).

[4] Shannon C. E . A mathematical theory of communication Bell System Technical Journal, vol. 27, pp. 385 (1984).

[5] Robert K. Dueck. Digital Design with CPLD Applications and VHDL. ISBN 1401840302 (2005).

[6] Vinod Kumar Khanna. Digital Signal Processing, (2009).

[7] Horowitz, Paul; Hill, Winfield. The Art Of Electronics, 2nd Ed. Cambridge University Press. pp. 471–473 (1989).

[8] Giuliano Benenti, Giulio Casati and Giuliano Strini, " Principles of Quantum Computation and Information" , World Scientific Publishing Co. Pte. Ltd, (2004).

[9] Nielsen, Michael A. Quantum computation and quantum information. Chuang, Isaac L. (10th anniversary ed.). Cambridge: Cambridge University Press (2011).

[10] Bokulich, Alisa; Jaeger, Gregg. Philosophy of Quantum Information and Entanglement. Cambridge University Press (2010).

[11] Hayashi, Masahito. Quantum Information Theory. Graduate Texts in Physics (2017).

[12] Preskill, John. "Lecture notes for physics." Quantum information and computation (1998).

[13] Mahan, Gerald D. Quantum Mechanics in a Nutshell. Princeton University Press (2008).

[14] Eleanor Rieffel and Wolfgang Polak " Quantum Computing" , Massachusetts Institute of Technology, QA76.889.R54, (2011).

[15] Joan Vaccaro. Quantum Computer Simulator, griffith.edu.au/joan/index.php (2013).

[16] Olivier Gazzano and Glenns S. Solomon, " Toward optical quantum information processing with quantum dots coupled to microstructures", Vol. 33, No. 7 / Journal of the Optical Society of America B, (2016

[17] Holevo, Alexander S. Statistical Structure of Quantum Theory. Lecture Notes in Physics. Springer. ISBN 3-540-42082-7 (2001).

[18] Busch, Paul . "Quantum States and Generalized Observables: A Simple Proof of Gleason's Theorem". Physical Review Letters. 91 (12): 120403 (2003).

[19] Kirkpatrick, K. A. "The Schrödinger-HJW Theorem". Foundations of Physics Letters. 19 (1): 95–102 (2006).

[20] Peres, Asher; Terno, Daniel R. "Quantum information and relativity theory". Reviews of Modern Physics. 76 (1): 93–123 (2004).

[21] Imre S., Gyongyosi L. Advanced Quantum Communications, an Engineering Approach, IEEE Press Editorial Board (2012).

[22] Alisa Bokulich, Gregg Jaeger. Philosophy of Quantum Information and Entanglement, Cambridge University Press (2010).

[23] Peng C.Z., J. Zhang, D. Yang, W.-B. Gao, H.-X. Ma, H. Yin, H.-P. Zeng, T. Yang, X.-B. Wang, and J.-W. Pa. Experimental long-distance decoy-state quantum key distribution based on

polarization encoding. Phys. Rev. Lett., 98:010505, BIBLIOGRAPHY (2007).

[24] Schmitt-Manderbach T., H.Weier, M. F¨urst, R. Ursin, F. Tiefenbacher, T. Scheidl, J. Perdigues, Z. Sodnik, C. Kurtsiefer, J. G. Rarity, A. Zeilinger, and H.Weinfurter. Experimental demonstration of free-space decoy-state quantum key distribution over 144 km. Phys. Rev. Lett., 98:010504 (2007).

[25] Ursin R., F. Tiefenbacher, T. Schmitt-Manderbach, H. Weier, T. Scheidl, M. Lindenthal, B. Blauensteiner, T. Jennewein, J. Perdigues, P. Trojek, B. ¨Omer, M. F¨urst, M. Meyenburg, J. Rarity, Z. Sodnik, C. Barbieri, H. Weinfurter, and A. Zeilinger. Entanglement-based quantum communication over 144 km. Nature Physics, 3:481, (2007).

[26] Gisin N., G. Ribordy, W. Tittel, and H. Zbinden. Quantum cryptography. Rev. Mod. Phys., 74:145, (2002).

[27] Briegel H. J., W. Dur, J. I. Cirac, and P. Zoller. Quantum repeaters: the role of imperfect local operations in quantum communication. Phys. Rev. Lett., 81:5932–5935, (1998).

[28] Duan L.M., M. D. Lukin, J. I. Cirac, and P. Zoller. Long-distance quantum communication with atomic ensembles and linear optics. Nature, 414:413–418, (2001).

[29] Bennett, C. H. and Brassard G., Quantum Cryptography: Public Key Distribution and Coin Tossing, Th. Comp. Sc., 560, 7–11, (2014).

[30] Bennett C. H. et al., "Teleporting an unknown quantum state via dual classical and Einstein-Podolsky-Rosen channels", Phys. Rev. Lett. 70,1895 (1993).

[31] Li-Nan Jiang, "Quantum Teleportation Under Different Collective Noise Environment" International Journal of Theoretical Physics (2018).

[32] Christian Mastromattei "Assessing the Practicality of a Simple Multinode Quantum Repeater" A thesis presented to the University of Waterloo in ful_llment of the thesis requirement for the degree of Master of Science in Physics, (2017).

[33] Dur W., Briegel H.-J., Cirac J. I., and Zoller P., Quantum repeaters based on entanglement purification, Phys. Rev. A, **59**:169–181, (1999).

[34] Deutsch D., Ekert A., Jozsa R., Macchiavello C., Popescu S., and Sanpera A., Quantum privacy amplification and the security of quantum cryptography over noisy channels, Phys. Rev. Lett., **77**:2818–2821, (1996).

[35] Bennett C. H., Brassard G., Popescu S., Schumacher B., Smolin J. A., and Wootters W. K., Purification of noisy entanglement and faithful teleportation via noisy channels, Phys. Rev. Lett, **76**:722–725, (1996).

[36] Zhao Bo, Robust and Efficient Quantum Repeater with Atomic Ensembles and Linear Optics, PhD Thesis, University of Heidelberg, Germany, July 16th, (2008).

[37] Cirac J. I., Zoller P., Kimble H. J., and Mabuchi H., Quantum state transfer and entanglement distribution among distant nodes in a quantum network, Phys. Rev. Lett., **78**:3221, (1997).

[38] Nadja K. Bernardes, and Peter van Loock. Hybrid quantum repeater with encoding, Phys. Rev A **86**, 052301 (2012).

[39] Wijdan M.K, Jawad A.H. Quantum Repeaters Based on Multiplexed Single-Photon Source, MSc Thesis, Institute of Laser for Postgraduate Studies. University of Baghdad, Iraq (2018).

[40] Luong D., Jiang L., Kim J., and Lutkenhaus N., Overcoming lossy channel bounds using a single quantum repeater node, Appl. Phys., B, **122** (4):96, (2016).

[41] Johannes B., Hannes P., Tim S., Mikhail D. Lukin, Peter L., Anders S. One-way quantum repeater based on near-deterministic photon-emitter interfaces. Phys. Rev. X 10, 021071 (2020).

[42] Krovi H., Guha S., Dutton Z., Joshua A., Slater C., Simon, and Tittel W., Practical Quantum Repeaters with Parametric Down-Conversion Sources, Appl. Phys. B, **122**, 3, 1-8 (2016).

[43] Pirandola S. and Laurenza R., General benchmarks for quantum repeaters, quantum-ph, **1512**.04945, (2016).

[44] Adnan N. Kadhim, Jawad A. Hasan, Wijdan M. Alkhalidy. Implementation of quantum repeater scheme based on non-identical quantum memories. Photonic Network Communications volume **39**, pages 39–46 (2020).

[45] Stefano Pirandola. Satellite quantum communications: Fundamental bounds and practical security. Phys. Rev. Research **3**, 023130 (2012).

[46] Boone K., J.-P. Bourgoin, E. Meyer-Scott, K. Heshami,1, T. Jennewein, and C. Simon. Entanglement over global distances via quantum repeaters with satellite links. quant-ph. 1410.5384v1(2014).

[47] Carlo Liorni, Hermann Kampermann & Dagmar Bruß. Quantum repeaters in space. *New J. Phys.* 23 053021 (2021).

[48] Mario Mastriani, Sundaraja Sitharama Iyengar. satellite quantum repeaters for a quantum Internet. Quantum engineering, Volume2, Issue4 (2020).

[49] Vergoossen et al. Satellite constellations for trusted node QKD networks. arXiv e-prints, page arXiv:1903.07845, Mar (2019).

[50] J. Yin et al. Satellite-to-ground entanglement based quantum key distribution. Phys. Rev. Lett., 119:200501, Nov 2017

[51] Pan J.W., Simon C., Brukner C., and Zeilinger A., Entanglement purification for quantum communication, Nature, **410**:1067–1070, (2001).

[52] Rozpdek F., Goodenough K., Ribeiro J., Kalb N., Caprara Vivoli V., Reiserer A., Hanson R., Wehner S., and Elkouss D., Parameter regimes for a single sequential quantum repeater, Quantum Sci. Technol. **3,** 034002, (2018).

[53] Chen Y.A., Chen S., Yuan Z.S., Zhao B., Chuu C.S., Schmiedmayer J., and Pan J.W., Memory-built-in quantum teleportation with photonic and atomic qubits, Nature Physics, **4:**103, (2008).

[54] Azuma K., Tamaki K., and Lo H. K., All photonic quantum repeaters, Nature Communications **6**, (2013).

[55] Van der Wal C. H., Eisaman M. D., Andr´e A., Walsworth R. L., Phillips D. F., Zibrov A. S., and Lukin M. D., Atomic memory for correlated photon states, Science, **301**:196–200, (2003).

[56] Matsukevich D. N., Chaneli`ere T., Jenkins S. D., Lan S.Y., Kennedy T.A.B., and Kuzmich A., Deterministic single photons via conditional quantum evolution, Phys. Rev. Lett., **97**:013601, (2006).

[57] Jin J., Grimau Puigibert M., Giner L., Slater J. A., Lamont M. R. E., Verma V.B., Shaw M. D., Marsili F., Nam S. W., Oblak D., and Tittel W., Entanglement swapping with quantum-memory-compatible photons, Phys. Rev. A **92**, 012329 (2015).

[58] Specht H. P., Nolleke C., Reiserer A., Upho M., Figueroa E., Ritter S., and Rempe G., A single-atom quantum memory, Nature, **473**,190-193, (2011).

[59] Blinov B.B., Moehring D.L., Duan L.M., and Monroe C., Observation of entanglement between a single trapped atom and a single photon, Nature, **428**,153-157, (2004).

[60] Childress L., Taylor J. M., Sorensen A. S., and Lukin M. D. Fault-tolerant quantum communication based on solid-state photon emitters, Phys. Rev. Lett., **96**:070504, (2006).

[61] Olmschenk S., Younge K. C., Moehring D. L., Matsukevich D. N., Maunz P., and Monroe C., Manipulation and detection of a trapped Yb+ hyperfine qubit, Phys. Rev. A, **76**:052314, (2007).

[62] Kuzmich A., Bowen W. P., Boozer A. D., Boca A., Chou C. W., Duan L.M., and Kimble H. J., Generation of non classical photon pairs for scalable quantum communication with atomic ensembles, Nature, **423**:731, (2003).

[63] Langer C., Ozeri R., Jost J. D., Chiaverini J., DeMarco B., Ben-Kish A., Blakestad R. B., Britton J., Hume D. B., Itano W. M., Leibfried D., Reichle R., Rosenband T., Schaetz T., Schmidt P. O., and Wineland D. J., Long-lived qubit memory using atomic ions, Phys. Rev. Lett., **95**:060502, (2005).

[64] Harty T. P., Allcock D. T. C., Balance C. J., Guidoni L., Janacek H. A., Linke N. M., Stacey D. N., and Lucas D. M., High-

fidelity preparation, gates, memory, and readout of a trapped-ion quantum bit, Phys. Rev. Lett., **113**:220501, (2014).

[65] Matsukevich D. N., Maunz P., Moehring D. L., Olmschenk S., and Monroe C., Bell inequality violation with two remote atomic qubits, Phys. Rev. Lett., **100**:150404, (2008).

[66] Kim T., Maunz P., and Kim J., Efficient collection of single photons emitted from a trapped ion into a single-mode fiber for scalable quantum-information processing, Phys. Rev. A, **84**:063423, (2011).

[67] Solano E., de Matos Filho R. L., and Zagury N., Deterministic bell states and measurement of the motional state of two trapped ions, Phys. Rev. A, **59**:R2539{R2543}, (1999).

[68] de Almeida N. G., All-quantum teleportation, Q. Phys, V **1**, (2017).

[69] Ljuić D. Z. Ivić. Influence of quantum lattice fluctuations on the stability of large polarons in anisotropic electron-phonon systems. Physical Review B 76, 052302 (2007).

[70] KUHLMEY B. T.,” Theoretical and Numerical Investigation of the Physics of Microstructured Optical Fibres”, PhD thesis, (2004).

[71] OFS Furukawa Company, “Understanding fiber optic attenuation” springer series,(2007).

[72] Ming M. –K.Liu, “Principles and Applications of – Optical Communication “, McGraw –Hill, 1996.

[73] Wong K., “Non Linear Optics in Photonic crystal fiber” MS.c thesis, 2003.

[74] Birks T.; D. M. Bird; T. D. Hedley;J. M. Pottage; and P.St. J. Russell, “Scaling laws and Vector effects in Bandgap Guiding Fibers” Optics Express ,Vol.12, pp. 69 -74, 2004.

[75] Elden, Metrologia, “Refractive index of air” Optics Express, Vol. 2 No.71, 1966.

[76] Jenkis F. and H. E. White, “Fundamentals of optics” McGraw – Hill, 3rd edition, 1957.

[77] Okamoto K., “Fundaments of optical waveguides” academic press, 2000.

[78] Agrawal P., “Nonlinear Fiber Optics,” Third Edition, 2001.

[79] Smith G. , J. Smolin. Additive extensions of a quantum channel. IEEE Information Theory Workshop Proceedings (2008).

[80] Charbon E., F. Sebastiano, A. Vladimirescu, H. Homulle, S. Visser, L. Song, R.M. Incandela. Cryo-CMOS for quantum computing. Proc. 2016 IEEE International Electron Devices Meeting (IEDM) (2016).

[81] Ladd TD, Jelezko F, Laflamme R, Nakamura Y, Monroe C, O'Brien JL. Quantum computers. Nature; 464: 45–53 (2010).

[82] Jobez P., Usmani I., Timoney N., Laplane C., Gisin N., and Afzelius M., Cavity-enhanced storage in an optical spin-wave memory, New J. of Phys., **16**, 083005, (2014).

[83] Khalif B.N., J. A. Hasan, R. S. Alhumaima, and H. S. Al-Raweshidy, Performance analysis of quantum based cloud radio access net- works, IEEE Access, vol. 8, pp. 18123 18133 (2019).

[84] Van Meter R., T. D. Ladd, W. J. Munro, and K. Nemoto, System design for a long-line quantum repeater, IEEE/ACM Transactionson Networking, vol. 17, no. 3, pp. 1002 1013 (2009).

[85] Alhumaima R.S, M. Khan, and H. S. Al-Raweshidy, Component and parameterised power model for cloud radio access network, IET Communications, vol. 10, no. 7, pp. 745 752 (2016).

[86] Cho Y.W., Campbell G. T., Everett J. L., Bernu J., Higginbottom D. B., Cao M. T., Geng J., Robins N. P., Lam P. K., and Buchler B. C., Highly efficient optical quantum memory with long coherence time in cold atoms, Optica **3**, 100-107 (2016).

[87] Lerch, Stefan; Bessire, Bänz; Bernhard, Christof; Feurer, Thomas; Stefanov, André . "Tuning curve of type-0 spontaneous parametric down-conversion". Journal of the Optical Society of America B. **30** (4): 953–958 (2013).

[88] Alhumaima R., M. Khan, and H. S. Al-Raweshidy, Component and parameterised power model for cloud radio access network, IET Communications, vol. 10, no. 7, pp. 745 752, (2016).

[89] Lucamarini, Marco, et al. "Overcoming the rate–distance limit of quantum key distribution without quantum repeaters." Nature 557.7705, 400-403 (2018).

[90] Auer, Gunther, et al. "How much energy is needed to run a wireless network?. IEEE wireless communications 18.5. 40-49 (2011).

[91] Shannon, Claude Elwood. "A mathematical theory of communication." ACM SIGMOBILE mobile computing and communications review 5.1 : 3-55 (2001).

[92] Al-Abbasi, Ziad Qais, and Daniel KC So. "Power allocation for sum rate maximization in non-orthogonal multiple access

system." 2015 IEEE 26th Annual International Symposium on Personal, Indoor, and Mobile Radio Communications (PIMRC). IEEE, (2015).

[93] Vu, Tung Thanh. "Energy efficiency maximization for downlink cloud radio access networks with data sharing and data compression." IEEE Transactions on Wireless Communications 17.8,4955-4970 (2018).

[94] Chen, Yan, et al. "Fundamental trade-offs on green wireless networks." IEEE Communications Magazine 49.6. 30-37 (2011).

[95] Dudi Y.O.n, L. Li, and A. Kuzmich. Light storage on the time scale of a minute. Physical Review A, 87:031801, (2013).

[96] Hsin Chen Yi, Meng-Jung Lee, I-Chung Wang, Shengwang Du, Yong-Fan Chen, Ying-Cheng Chen, and Ite A. Yu. Coherent optical memory with high storage efficiency and large fractional delay. Physical Review Letters, 110:083601, (2013).

[97] Xiao-Hui Bao, Andreas Reingruber, Peter Dietrich, Jun Rui, Alexander Duck, Thorsten Strassel, Li Li, Nai-Le Liu, Bo Zhao, and Jian-Wei Pan. Efficient and long-lived quantum memory with cold atoms inside a ring cavity. Nature Physics, 8: 517, (2012).

[98] Radnae A.Gv, Y. O. Dudin, R. Zhao, H. H. Jen, S. D. Jenkins, A. Kuzmich, and T. A. B. Kennedy. A quantum memory with telecom-wavelength conversion. Nature Physics, 6:894, (2010).

الملخص

تعاني عملية ارسال المعلومات لمسافات طويلة سواء عن طريق الكيبل البصري او الفضاء المفتوح من مشكلة اضمحلال الاشارة، ولتجاوز هذه المشكلة تم استحداث المكرر الكمومي. في هذه البحث تم دراسة تأثير كل من (Decoherence time) وكفاءة إدخال الفوتونات في الكيبل البصري على كفاء أداء المكرر الكمومي، كما تم اجراء مقارنة بين أداء النظام الكمومي والنظام الهجين (تقليدي مع كمومي)، ولتحقيق هدف البحث تم استخدام ثلاثة أنواع من الذاكرة الكمومية وبخصائص مختلفة في كل من المكرر الكمومي المفرد وكذلك المتعدد المقاطع. وقد بينت النتائج التي توصلت لها الدراسة ان زيادة (Decoherence time) يؤدي الى زيادة المسافة التي من الممكن ان تصل اليها الاشارة المرسلة في كلا النوعين من المكرر الكمومي وبدون أي تأثير على مقدار الاشارة المرسلة، اذ تبين انه اذا كانت قيمة (T_2= 16 s) فان المسافة التي من الممكن تصل اليها الاشارة حوالي (900 كم) بينما اذا كانت قيمة (T_2= 0.018 s) فان المسافة سوف تقل الى حوالي (400 كم)، فيما كان تأثير زيادة وكفاءة إدخال الفوتونات في الكيبل البصري على كل من المسافة ومقدار الاشارة المرسلة، واخيراً أثبتت نتائج المقارنة تشير نتائج المقارنة بين الأنظمة الكمومية والأنظمة الهجينة إلى أن حالة النظام الكمومي سجلت معدل بت أعلى لأن قناتها بصرية بحتة أو لاسلكية ذات عرض نطاق مرتفع، مما يزيد من معدل البيانات. في الحالة الهجينة ، كان جزءًا من القناة عبارة عن شبكة لاسلكية كلاسيكية، والتي تتميز بنطاق ترددي أقل من جميع الحالات الكمومية. أخيرًا، تحتوي الحالة الكلاسيكية على تردد وعرض نطاق أقل مما يفرض على معدل البيانات أن يصبح الأقل. أيضًا، تُظهر النتيجة التي تم الحصول عليها أن الأنظمة الهجينة قد توفر تأخيرًا أقل، وصيانة أقل وقابلية للتوسع إلى أقصى حد.

وزارة التعليم العالي والبحث العلمي
جامعة بغداد
معهد الليزر للدراسات العليا

دراسة مقارنة للمكررات الكمومية

رسالة مقدمة الى

معهد الليزر للدراسات/جامعة بغداد/لاستكمال متطلبات الدراسة نيل شهادة الماجستير

من قبل

مروى حميد كاظم

بكالوريوس هندسة الاتصالات / 2007

إشراف

الدكتور جواد عبد الكاظم حسن

2021م **1442هـ**